GLIA

WILEY

RESEARCH ARTICLE

Adenosine receptors are the on-and-off switch of astrocytic cannabinoid type 1 (CB1) receptor effect upon synaptic plasticity in the medial prefrontal cortex

Joana Gonçalves-Ribeiro[1,2] | Oksana K. Savchak[1,2] | Sara Costa-Pinto[1,2] |
Joana I. Gomes[1,2] | Rafael Rivas-Santisteban[3,4] | Alejandro Lillo[3,4] |
Javier Sánchez Romero[5,6] | Ana M. Sebastião[1,2] | Marta Navarrete[5] |
Gemma Navarro[3,4,7] | Rafael Franco[4,8,9] | Sandra H. Vaz[1,2]

[1]Instituto de Farmacologia e Neurociências, Faculdade de Medicina, Universidade de Lisboa, Lisbon, Portugal

[2]Instituto de Medicina Molecular João Lobo Antunes, Faculdade de Medicina, Universidade de Lisboa, Lisbon, Portugal

[3]Department of Biochemistry and Physiology, School of Pharmacy and Food Science, Universitat de Barcelona, Barcelona, Spain

[4]CiberNed, Network Center for Neurodegenerative Diseases, National Spanish Health Institute Carlos III, Madrid, Spain

[5]Instituto Cajal, CSIC, Madrid, Spain

[6]PhD Program in Neuroscience, Universidad Autónoma de Madrid-Instituto Cajal, Madrid, Spain

[7]Institut de Neurociències, Universitat de Barcelona, Barcelona, Spain

[8]Molecular Neurobiology Laboratory, Department of Biochemistry and Molecular Biomedicine, Faculty of Biology, Universitat de Barcelona, Barcelona, Spain

[9]School of Chemistry, Universitat de Barcelona, Barcelona, Spain

Correspondence
Sandra H. Vaz, Instituto de Farmacologia e Neurociências, Faculdade de Medicina, Universidade de Lisboa, Lisbon, Portugal.
Email: svaz@medicina.ulisboa.pt

Abstract

The medial prefrontal cortex (mPFC) is involved in cognitive functions such as working memory. Astrocytic cannabinoid type 1 receptor (CB1R) induces cytosolic calcium (Ca^{2+}) concentration changes with an impact on neuronal function. mPFC astrocytes also express adenosine A_1 and A_{2A} receptors (A_1R, $A_{2A}R$), being unknown the cross-talk between CB1R and adenosine receptors in these cells. We show here that a further level of regulation of astrocyte Ca^{2+} signaling occurs through CB1R-$A_{2A}R$ or CB1R-A_1R heteromers that ultimately impact mPFC synaptic plasticity. CB1R-mediated Ca^{2+} transients increased and decreased when A_1R and $A_{2A}R$ were activated, respectively, unveiling adenosine receptors as modulators of astrocytic CB1R. CB1R activation leads to an enhancement of long-term potentiation (LTP) in the mPFC, under the control of A_1R but not of $A_{2A}R$. Notably, in IP3R2KO mice, that do not show astrocytic Ca^{2+} level elevations, CB1R activation decreases LTP, which is not modified by A_1R or $A_{2A}R$. The present work suggests that CB1R has a homeostatic role on mPFC LTP, under the control of A_1R, probably due to physical crosstalk between these receptors in astrocytes that ultimately alters CB1R Ca^{2+} signaling.

1 | INTRODUCTION

Astrocytes tightly and dynamically interact with synapses having a critical role in synaptic information processing (Araque et al., 1999; Araque et al., 2014; Durkee & Alfonso, 2019; Guerra-Gomes et al., 2018; Perea et al., 2009; Perea & Araque, 2005), ultimately playing a critical function in cognitive (Kofuji & Araque, 2021), anxiety (Cho et al., 2022) and depressive-like behavior (Banasr & Duman, 2008). A key step in the interaction between astrocytes and neurons is the calcium (Ca^{2+})-dependent release of gliotransmitters, such as glutamate (de Ceglia et al., 2023; Navarrete & Araque, 2008; Perea et al., 2016), ATP (Gordon et al., 2005; Hatashita et al., 2023; Xiong et al., 2018), GABA (Le Meur et al., 2012), and D-serine (Abreu et al., 2023; Henneberger et al., 2010; Robin et al., 2018), which in turn is triggered by a wide variety of membrane receptors for neurotransmitters and neuromodulators, including glutamate (Skowrońska et al., 2019), ATP (Baraibar et al., 2023; Jacob et al., 2014), GABA (Jiménez-Dinamarca et al., 2022; Le Meur et al., 2012), and endocannabinoids (eCBs) receptors, among others (Corkrum et al., 2020; Perea et al., 2009; Volterra & Meldolesi, 2005).

The eCBs, acting through the activation of the cannabinoid type one receptor (CB1R), are among the most ubiquitous signaling molecules in the central nervous system (CNS). In neurons, CB1R is coupled with $G_{i/o}$ proteins, and their activation leads to a reduction of neurotransmitter release (Howlett, 2005), while in astrocytes the activation of CB1R induces an intracellular Ca^{2+} increase (Lauckner et al., 2005) thus triggering the astrocyte-to-neuron neuromodulatory loop mentioned above. The role of eCBs and astrocytic CB1R in the hippocampus, namely their ability to modulate heterosynaptic potentiation (Navarrete & Araque, 2010), long-term synaptic plasticity (LTP) (Gómez-Gonzalo et al., 2015) and hippocampal long-term depression (LTD) (Han et al., 2012), is well known. Astrocytic CB1R is also known to be necessary for the consolidation of long-term object recognition memory, via a mechanism involving D-serine supply to synaptic NMDAR (Robin et al., 2018). In neocortical synapses, astrocytic CB1R controls the spike timing-dependent depression (Min & Nevian, 2012) and the heteroneuronal synaptic depression (Baraibar et al., 2023) but much less is known about their ability to affect synaptic plasticity in the medial prefrontal cortex (mPFC).

The gliotransmitter ATP is extracellularly converted into adenosine, which by itself is a modulator of neuronal as well as astrocytic activity. Adenosine acts through high-affinity inhibitory A_1 (A_1R) and facilitatory A_{2A} ($A_{2A}R$) receptors to modulate synaptic transmission and plasticity (Gomes et al., 2021). Functional A_1R and $A_{2A}R$ heteromers are found in astrocytes (Cristóvão-Ferreira et al., 2013), while the heteromerization of these receptors with CB1R was so far only studied in neurons (Moreno et al., 2017). CB1R and $A_{2A}R$ co-localize in striatal glutamatergic terminals, being the depressive CB1R action upon motor activity counteracted by $A_{2A}R$ blockade (Carriba et al., 2007; Ferré et al., 2010). Additionally, the CB1R-mediated effect in the striatum is significantly reduced in rats with neuronal overexpression of $A_{2A}R$ (Chiodi et al., 2016), suggesting that the upregulation of $A_{2A}R$, known to occur during aging (Batalha et al., 2012), may lead to a decrease in cannabinoid signaling possibly through the dampening of A_1R (Ferré & Sebastião, 2016) signaling that is mediated by $A_{2A}R$ ligands. Furthermore, hippocampal LTP and memory deficits induced by acute and chronic CB1R activation are also modulated by $A_{2A}R$ (Mouro et al., 2017, 2019) and A_1R (Sousa et al., 2011), although no significant change was observed in the LTP decrease induced by the CB1R blockade in the A_1R knockout mice (Silva-Cruz et al., 2017). Even though there are several studies on the $A_1R/A_{2A}R$ crosstalk with CB1R in neurons, it is surprising that no study has so far addressed $A_1R/A_{2A}R$ crosstalk with CB1R in astrocytes.

The mPFC is deeply involved in cognitive and executive functions such as decision-making, working memory, and attention (Blum et al., 2006; Euston et al., 2012; Gabbott et al., 2005). Astrocytes play a key role in the mPFC circuitry since the compromised astrocytic function in this area leads to anhedonia and altered cognitive function (Banasr & Duman, 2008; Lima et al., 2014), compromised cognitive flexibility along with altered delta, alpha, and gamma power (Brockett et al., 2018) and impaired GABAergic signaling (Mederos et al., 2021). Furthermore, mPFC layer II/III-V LTD is CB1R-dependent (Lafourcade et al., 2007) and the overexpression of CB1R in this area leads to decreased social behavior and an increased social withdrawal (Klugmann et al., 2011). However, a low dose of WIN-55,212, a CB1R agonist (Bambico et al., 2007) decreases immobility time in the forced swim test. These data reveal an important role of CB1R for the mPFC circuitry, however, remains to be discriminated the impact of astrocytic CB1R on synaptic plasticity in this brain region.

Focusing, therefore, upon the mPFC, we aimed to unveil the role of astrocytic CB1R and its crosstalk with adenosine receptors (ADOR) to modulate synaptic transmission and plasticity. We studied the A_1R-CB1R and $A_{2A}R$-CB1R interaction at three levels: (i) the presence of A_1R-CB1R and $A_{2A}R$-CB1R heteromers in astrocytes and how they are modulated by endogenous adenosine; (ii) the impact of ADOR modulation upon astrocytic CB1R-mediated Ca^{2+} transients and (iii) the effect A_1R-CB1R and $A_{2A}R$-CB1R crosstalk upon synaptic plasticity of the mPFC. To understand the relative role of astrocytic versus neuronal type CB1R, we used the inositol 1,4,5-trisphosphate receptor type 2 knockout (IP3R2KO) mouse model (Srinivasan et al., 2015), which lacks Ca^{2+} elevations solely in astrocytes. In this model, CB1R-mediated Ca^{2+}-signaling is thus absent while preserving the action of CB1R in other cell types. Our results show, for the first time, that CB1R heterodimerizes with A_1R or $A_{2A}R$ in astrocytes, and that the level of activation of ADOR influences the CB1R-dependent Ca^{2+} signaling in these cells. Furthermore, we observed that the

modulatory action of CB1R upon synaptic plasticity in the mPFC is A_1R-dependent only when the astrocytic Ca^{2+} signaling is preserved.

2 | RESULTS

2.1 | $A_{2A}R$ and A_1R heteromerized with CB1 receptors in astrocytes in an adenosine-dependent manner

Although there are reports of a direct interaction between ADOR and CB1R in neurons (Carriba et al., 2007; Chiodi et al., 2016; Ferré et al., 2010), nothing is known regarding this type of interaction in astrocytes. Thus, we evaluated the direct interaction between ADOR with CB1R in astrocytes in culture by performing bioluminescence resonance energy transfer (BRET) and proximity ligation assay (PLA). The partner receptors were the $A_{2A}R$ or the A_1R and the CB1R, for which cDNA constructs of fusion proteins containing the human

full-length version and either Rluc or YFP were obtained. The cDNAs coding for either A_1RRLuc or $A_{2A}RRluc$ and CB1R-YFP were transfected into cultured astrocytes, and the immunocytochemical studies were performed as indicated in Material and Methods. For both pairs of receptors evaluated, $A_{2A}RRluc$/CB1R-YFP and A_1RRluc/ CB1R-YFP, a saturable BRET curve was observed, with values of $BRET_{max}$ of 15.4 mBU and a $BRET_{50}$ of 2.9 for A_1R-CB1R (Figure 1a1), and of BRETmax of 37.3 mBU and a $BRET_{50}$ of 2.4 for $A_{2A}R$-CB1R (Figure 1a2), which is indicative of direct interaction between CB1R with A_1R or $A_{2A}R$. The negative control was performed by replacing the $A_1R/A_{2A}R$-RLuc with D_1R-RLuc which led to a linear nonspecific BRET signal in astrocyte primary cultures (Figure 1a1,a2). D_1R-RLuc was used as nonspecific BRET signal since there is no evidence of CB1-D1 receptors heteromerization reported so far. To complement our results, an in situ proximity ligation assay (PLA) was performed. PLA is a molecular method that allows the detection of endogenous protein–protein interactions, by identifying complexes formed by two proteins, including
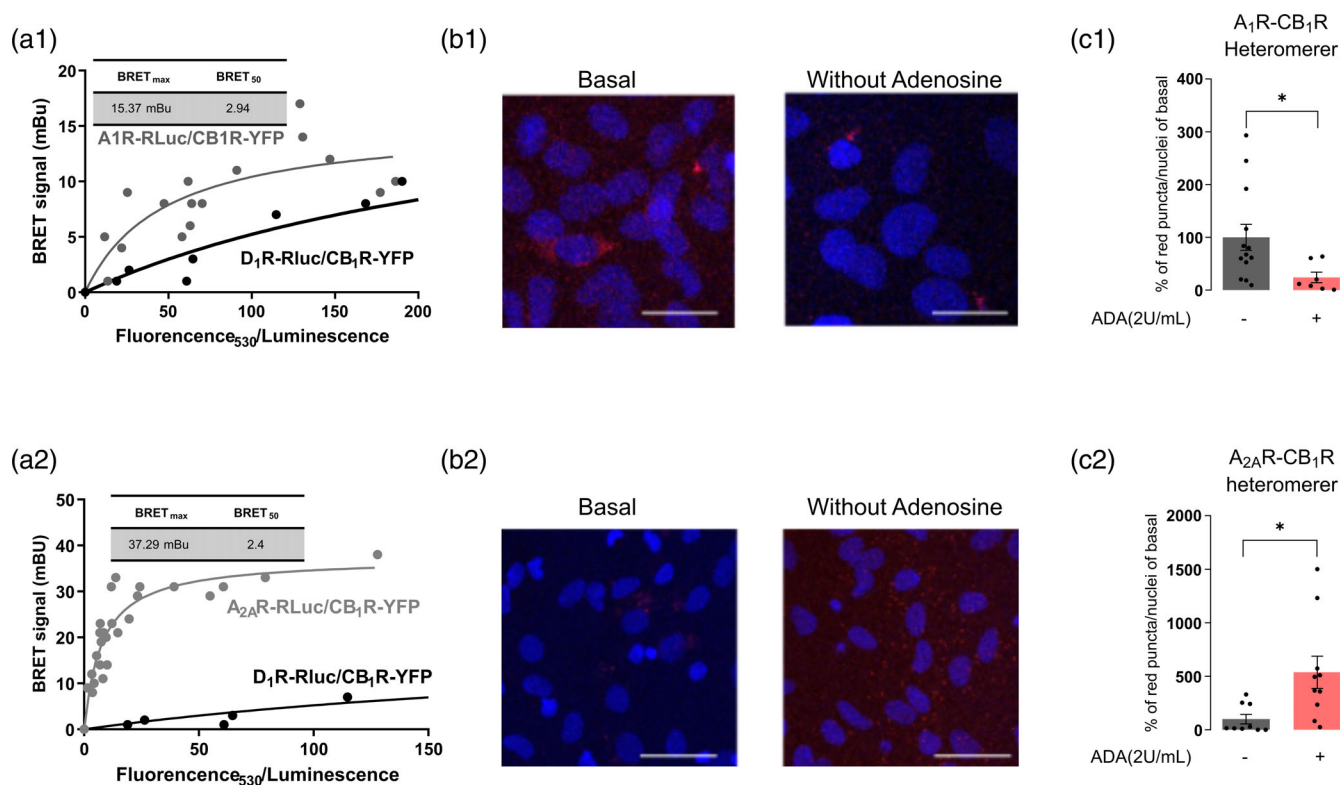
FIGURE 1 A2AR-CB1R and A1R-CB1R heteromer in cortical astrocytes. (a) BRET saturation experiments were developed in primary culture of astrocytes transfected with a constant amount of cDNAs for either A1RcRluc (3 μg) (a1) or A2ARnRluc (3 μg) (a2), and increasing amounts of cDNAs for CB1RnYFP (0.6 to 6 μg) (see methods for further details). D1R-Rluc cDNA (3 μg) and increasing amounts of cannabinoid CB1 receptor-YFP cDNA (0.2–4 μg) were used to provide a negative control. Net BRET (in milli BRET units) is plotted against the ratio: net YFP fluorescence/luminescence; net YFP fluorescence (530 nm) is obtained by subtracting from the total value of 530 nm readings the autofluorescence of cells expressing the donor protein but not the YFP-containing acceptor. (b) A proximity ligation assay (PLA) was performed in the primary culture of astrocytes, using specific primary antibodies against CB1R and A1R (b1) or A2AR (b2). Representative confocal microscopy images (stacks of 4 consecutive planes) show heteroreceptor complexes as red clusters and Hoechst-stained nuclei (blue). Scale bar: 20 μm. (c) Summary plot of percentage of red dots/cell for CB1R-A1R heteromers (c1) and CB1R-A2AR heteromers (c2) in absence or presence of adenosine deaminase (ADA, 2 U/mL), as indicated in the bottom of the plots, using astrocytes cultures with 3 weeks old. The number of red dots/ cells was quantified using a Duolink Image tool (Andy's Algorithm). Data are the mean ± SEM of three independent experiments performed in triplicate. *$p < .05$ assessed by unpaired Student's *t* test.

brain sections (Borroto-Escuela et al., 2016) or in cell cultures (Franco et al., 2019). Cortical primary astrocytes were treated with selective antibodies against A_1R, $A_{2A}R$, and CB1R (Figure 1b1,b2) to evaluate the receptor complex expression by measuring the number of fluorescence red puncta surrounding the Hoechst-stained nucleus which corresponds to clusters of heteroreceptor complexes, either A_1R-CB1R (Figure 1b1) or $A_{2A}R$-CB1R (Figure 1b2). We observed that the removal of extracellular adenosine using adenosine deaminase (ADA, 2 U/mL), an enzyme that catalyzes the irreversible deamination of adenosine to inosine, led to a significant decrease of red puncta/cell of about 76% when compared to the control (A_1R-CB1R$_{(without\ ADA)}$: 100 ± 24.7%, A_1R-CB1R$_{(with\ ADA)}$: 24.2 ± 10.12%, unpaired Student's t test: $t_{18} = 2.175$, $p = .043$) (Figure 1b1,c1) for the A_1R-CB1R receptor complex, while for the $A_{2A}R$-CB1R heteromer complex was observed a significant increase of the red puncta/cell in presence of ADA ($A_{2A}R$-CB1R$_{(without\ ADA)}$: 100 ± 44.82%, $A_{2A}R$-CB1R$_{(with\ ADA)}$: 538.1 ± 150.3%, unpaired Student's t test: $t_{17} = 2.664$, $p = .0164$) (Figure 1b2,c2). Moreover, we also performed an in situ PLA in HEK cells to evaluate the possible D1R-CB1R complex expression. We did not observe any red puncta/cell, which confirmed that CB1R and D1R are not able to form heteromers (Figure S1). Altogether, these data indicate that the CB1R heteromerization with A_1R or $A_{2A}R$ depends on the levels of extracellular adenosine.

2.2 | CB1R-mediated Ca^{2+} signaling in astrocytes is modulated by adenosine receptors

Although astrocytic primary cultures are relevant for research it is important to acknowledge that these cultures may sometimes exhibit altered proteomics and genomics compared to _ex vivo_ astrocytes (Lange et al., 2012). Thus, before investigating the adenosinergic influence in CB1R-mediated Ca^{2+} signaling, we confirmed if CB1R-mediated Ca^{2+} in primary cultures of astrocytes is in line with _ex vivo_ astrocytes (Navarrete & Araque, 2008). To accomplish this, we used ACEA, a selective CB1R agonist. During the time course of the Ca^{2+} imaging experiment (Figure 2a2) we obtained images of relative fluorescence for 340 and 380 nm, from which the 340 of 380 ratio was determined (Figure 2a3). Thus, to confirm its Gq- and PLC-dependency in cultures, pharmacological bath application was employed and frequency of Ca^{2+} events in these cells was accessed (Figure S2A). ACEA effect was dose-dependent (Figure S2B–D,G) and abolished with CB1R inverse agonist, AM251 (1 μM) (Figure S2E–G). This mechanism also revealed to be PLC dependent (Figure S2E–G) and driven from intracellular Ca^{2+} stores within the endoplasmic reticulum (ER) (Figure S2E,F3), as evidenced by its blockade in the presence of α-CPA, a reversible inhibitor of Ca^{2+}-ATPases, that depletes intracellular Ca^{2+} stores. Additionally, when cells were incubated in a low Ca^{2+} medium (0.5 mM $CaCl_2$ + 1 mM EGTA) throughout the whole experiment, the signaling persisted (Figure S2E,F4) but at a significantly attenuated frequency (ACEA: 0.96 ± 0.11 transients per 5 min and ACEA $_{(low\ calcium)}$: 0.32 ± 0.11 transients per 5 min, $p < .01$)

(Figure S2E,F4). Taken together, these results suggest that _in vitro_ CB1R signaling is similar to _ex vivo_.

Adenosine receptors are not able to elicit Ca^{2+} transients but they can modulate the response of other receptors (Alloisio et al., 2004; Hashmi et al., 2007; Ribeiro et al., 2002). Having in mind our previous observation, that A_1R and $A_{2A}R$ physically interact with CB1R in astrocytes, we next hypothesized that ADOR modulates the known CB1R-mediated Ca^{2+} signaling in astrocytes (Navarrete & Araque, 2008). To evaluate the influence of ADOR modulation upon CB1R-mediated Ca^{2+} signaling in astrocytes, Ca^{2+} imaging experiments were performed using primary astrocyte cultures, and the amplitude of the Ca^{2+} transients was measured after a focal application of ACEA (Figure 2a1). To avoid endogenous adenosine affecting adenosine receptors expressed in the cells, which can interfere with the activation of the pathway of interest (Cristóvão-Ferreira et al., 2013; Lopes et al., 1999), all following experiments were performed with cells incubated with ADA (2 U/mL) (Figure 2a2). In the absence of extracellular adenosine, the focal application of ACEA (500 μM), induced Ca^{2+} transients with an average amplitude of 1.45 ± 0.07 which showed no significant difference from the control situation, without ADA incubation, with an average amplitude of 1.63 ± 0.13 (unpaired Student's t test: $t_{24} = 1.046$, $p = .3058$, $n = 13$ cells from 4 independent cultures) (Figure 2b1,b2). A puff application of Ca^{2+}-HEPES buffer did not generate any Ca^{2+} transients (Figure 2b1,b2).

To unveil the impact of A_1R modulation upon CB1R-mediated Ca^{2+} signaling, cells were incubated with the selective A_1R agonist, CPA (30 nM). An ACEA puff in the presence of CPA led to a significant increase of the CB1R-mediated Ca^{2+} amplitude when compared with ACEA puff application without the activation of A_1R ($Ca^{2+}T_{(ADA+CPA)}$: 2.07 ± 0.32 vs. $Ca^{2+}T_{(ADA)}$: 1.47 ± 0.25, one-way ANOVA: $F_{(2,34)} = 20.73$, $p < .0001$) (Figure 2c1,c2e). The facilitatory action of CPA upon ACEA-mediated Ca^{2+}-signaling was lost when cells were previously incubated with the selective A_1R antagonist, DPCPX (50 nM) ($Ca^{2+}T_{(ADA+CPA+DPCPX)}$:1.37 ± 0.31, $p < .0001$) (Figure 2c1, c2,e), further supporting the evidence that A_1R activation positively modulates CB1R-mediated astrocytic Ca^{2+} signaling. As for the influence of $A_{2A}R$ modulation upon CB1R-mediated Ca^{2+} signaling, cultured astrocytes were incubated with the selective $A_{2A}R$ agonist, CGS 21680 (30 nM). The $A_{2A}R$ activation lead to a significant decrease of CB1R elicited Ca^{2+} transient amplitude ($Ca^{2+}T_{(ADA+CGS)}$: 1.24 ± 0.18 vs. $Ca^{2+}T_{(ADA)}$:1.47 ± 0.07, one-way ANOVA: $F_{(2,38)} = 23.404$, $p = .0375$) (Figure 2d1,d2,e), an effect that was counteracted by the selective antagonism of $A_{2A}R$, Scheme 58261 (50 nM) ($Ca^{2+}T_{(ADA+SCH+CGS)}$:1.42 ± 0.11), showing that $A_{2A}R$ downregulates CB1R-mediated Ca^{2+} signaling in astrocytes. Furthermore, to investigate adenosinergic influence in Ca^{2+} signaling kinetics, a computational analysis was employed previously described in literature (Lopes et al., 2023). Prior to CB1R activation, $A_{2A}R$ activation was shown to elevate baseline Ca^{2+} levels (Figure S3A) consistent with previous reports (Kanno & Nishizaki, 2012) while no significant differences were observed either in rise or decay slopes (Figure S3B,C) for all pharmacology used.
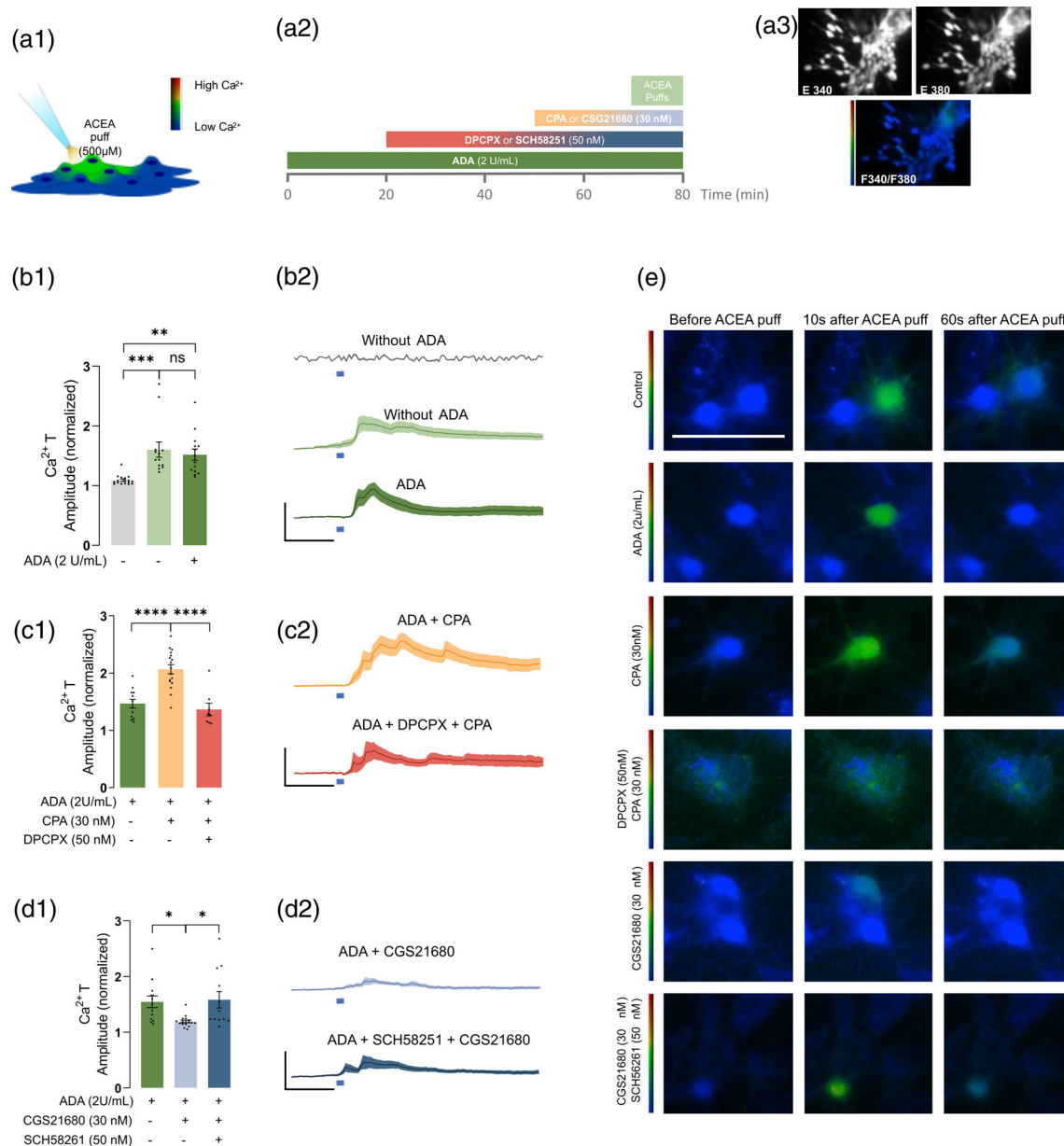
FIGURE 2 Modulation of astrocyte Ca^{2+}-signaling by A2AR-CB1R and A1R-CB1R heteromers. (a1) Illustration of the CB1R-mediated Ca^{2+} transient elicited by a puff application of ACEA (500 μM), a selective CB1R agonist. In the absence or presence of the indicated drugs, a local application of ACEA in Ca^{2+}-HEPES buffer was made. ACEA-induced Ca^{2+} transients in astrocytes near the puff application. (a2) Timeline of the CB1-mediated Ca^{2+} signaling experiments. (a3) Representative images obtained during a Ca^{2+} imaging experiment of relative fluorescence for 340 and 380 nm, and for the 340/380 ratio. Scale bar: 20 μm. (b1) Summary plot illustrating the negative control (Ca^{2+}-HEPES puff) and the absence of effect of adenosine deaminase (ADA) on the Ca^{2+} response amplitude to ACEA (500 μM) puff in astrocytes. (b2) Representative traces of the Ca^{2+} transients induced by Ca^{2+}-HEPES (top panel) ACEA (500 μM) puff application under control condition (middle panel) and after incubation for 20 min with ADA (2 U/mL) (bottom panel). (c1) Summary plot showing the effect of ACEA (500 μM) puff on the Ca^{2+} response amplitude in astrocytes in the absence or presence of CPA (30 nM) (20 min before the ACEA puff) and DPCPX (50 nM) (30 min prior to puff or incubation of CPA). These experiments were performed in the presence of ADA (2 U/mL). (c2) Representative traces of the Ca^{2+} transients induced by ACEA (500 μM) puff application after incubation for at least 20 min with ADA (2 U/mL) and CPA (30 nM) (top panel) and after incubation for at least 20 min with ADA (2 U/mL), CPA (30 nM) and DPCPX (50 nM) (bottom panel). (d1) Summary plot showing the effect of ACEA (500 μM) puff on the Ca^{2+} response amplitude in astrocytes in the absence or presence of CGS 21680 (30 nM) (20 min prior to puff) and SCH58251 (50 nM) (30 min prior to puff or incubation of CGS21680). These experiments were performed in the presence of ADA (2 U/mL). (d2) Representative traces of the Ca^{2+} transients induced by ACEA (500 μM) puff application after incubation for at least 20 min with ADA (2 U/mL) and CGS21680 (30 nM) (top panel) and after incubation for at least 20 min with ADA (2 U/mL), CGS21680 (30 nM) and SCH58261 (50 nM) (bottom panel). The Ca^{2+}-HEPES puff application is indicated in the panel (b2) by the gray line. The ACEA (500 μM) puff application is indicated in the panels (b2), (c2), and (d2) by the blue line. (e) Representative Ca^{2+} imaging images before (right panels), 10 s after (middle panels), and 60 s after (left panels) ACEA (500 μM) puff application with the different tested drugs as indicated: ADA (2 U/mL), CPA (30 nM), DPCPX (50 nM), CGS21680 (30 nM) and SCH5861 (50 nM). Scale bar: 20 μm. Data are expressed as mean ± SEM of 10–19 responsive cells from 4 independent cultures of astrocytes. *$p < 0.05$, **$p < 0.01$, **$p < 0.001$, ****$p < .0001$ assessed by one-way A-NOVA followed by Bonferroni correction.

2.3 | CB1R has a dual action upon mPFC synaptic plasticity, which is astrocytic Ca^{2+} signaling-dependent

In order to evaluate the impact of CB1R heteromerization with A_1R or $A_{2A}R$ upon synaptic plasticity in the mPFC we moved from an *in vitro* to an *ex vivo* model, the IP3R2KO mice that lack astrocytic Ca^{2+} signaling. Although there are still Ca^{2+} events in IP3R2KO mice (Sherwood et al., 2017) it is widely accepted that in IP3R2KO mice the bulk/somatic Ca^{2+} responses (Petravicz et al., 2008) are virtually absent. Prior to clarifying the role of CB1R in the mPFC, the initial objective was to characterize this animal model, specifically focusing on synaptic plasticity within this brain region. To induce LTP, high-frequency stimulation (HFS) was applied to layer II/III neurons of the mPFC (Figure 3a), and field excitatory postsynaptic potentials

(fEPSPs) were recorded in layer V as previously reported (Fénelon et al., 2011; Gemperle et al., 2003; Kerkhofs et al., 2018; Tanqueiro et al., 2021). The HFS stimulation protocol induced an LTP magnitude quantified as the % change in the average slope of the fEPSP before and 40–50 min after HFS stimulation (see Methods). Noticeable, LTP magnitude was significantly higher in IP3R2KO mice than in IP3R2WT mice (IP3R2WT$_{(CTL)}$: 43.2 ± 9.35%; IP3R2KO$_{(CTL)}$: 93.9 ± 7.86%, $n = 7-11$, unpaired Student t test, $p = .0008$) (Figure 3b1–b3). Given that astrocytes can release the inhibitory neurotransmitter GABA (Lee et al., 2010) in a Ca^{2+}-dependent manner, and considering the well-established role of this GABA in the tonic inhibition of circuits (Goenaga et al., 2023), we hypothesized that the absence of IP3R2-mediated Ca^{2+} signaling might contribute to the observed increase in LTP. To test this hypothesis, we conducted whole-cell patch-clamp recordings of miniature inhibitory postsynaptic currents (mIPSCs) in layer V neurons (Figure 3a),
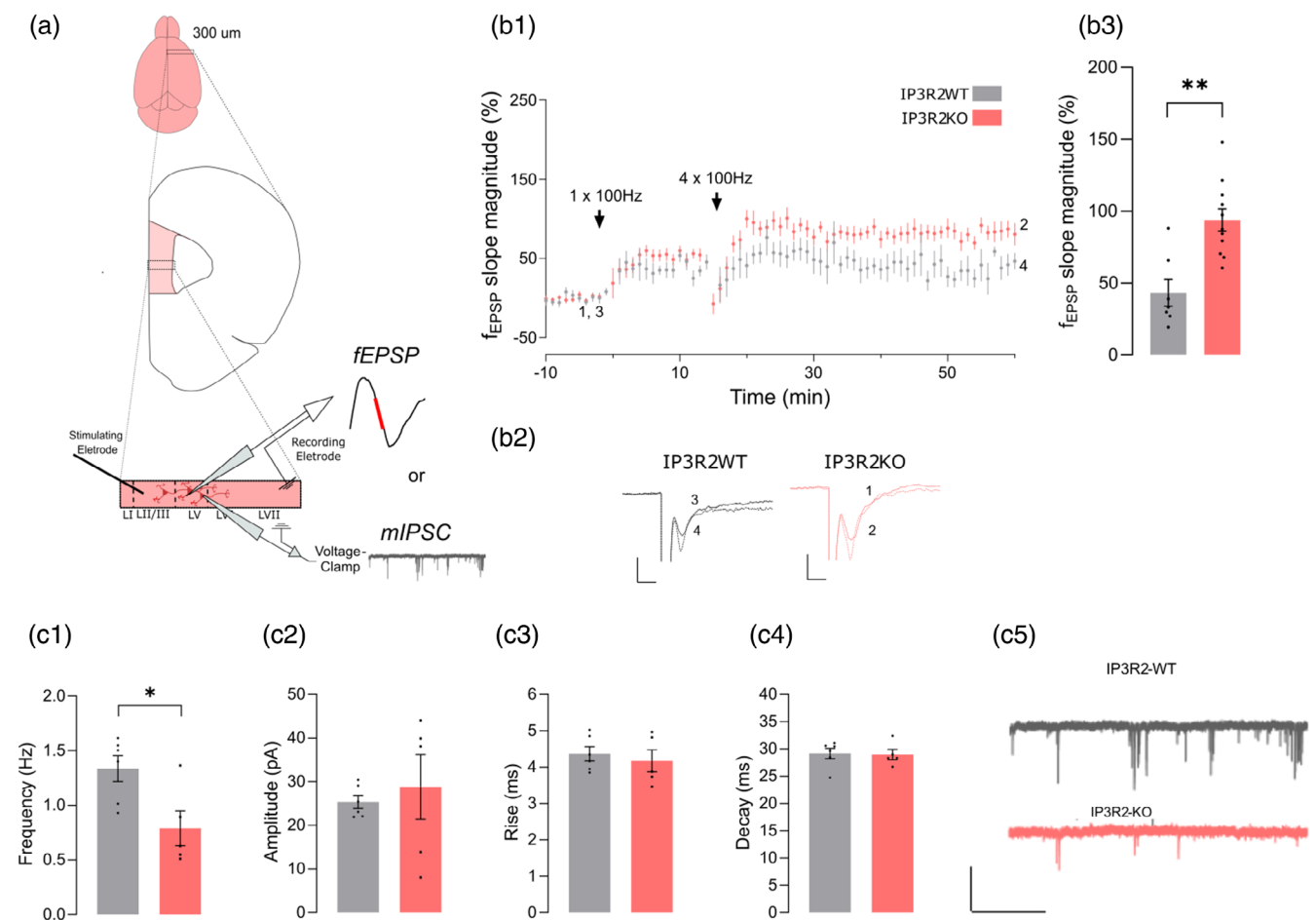
FIGURE 3 IP3R2KO present a higher LTP and lower tonic inhibition. (a) Illustration of recording configuration. Positioning of the stimulating (layer 2/3 mPFC) and recording electrodes (layer 5 mPFC) and schematic representation of the recorded potential and of the mIPSC. (b) Time course of mPFC layer V LTP, triggered by a priming train of high-frequency stimulation (HFS), followed 15 min later by four HFS trains (50 pulses at 100 Hz, 0.5 s duration, delivered every 10 s), in brain slices from IP3R2WT (black) and IP3R2KO mice (red). (b2) Representative traces of fEPSPs (preceded by the stimulus artifact and the pre-synaptic volley) recorded before (1 and 3, dashed line) and after (2 and 4, continuous line) inducing LTP in slices from IP2R2WT (1 and 2) or IP3R2KO (3 and 4) mice; tracings recorded from the same slice are superimposed. Comparison of mIPSCs frequency (c1), amplitude (c2), rise (c3), and decay (c4) in IP3R2WT (gray) and IP3R2KO (pink). (c5) Representative traces of mIPSCs in IP3R2WT and IP3R2KO, scale bar: 50 pA, 5 s. (see methods for further details). For experiments in (B), data are expressed as mean ± SEM of 7–11 slices per condition. **$p < .01$ assessed by unpaired Student's t test. For experiments in (c), data are expressed as mean ± SEM of 5–6 neurons from 3 to 5 animals, *$p < .05$ assessed by unpaired Student's t test.

as these currents are highly correlated with tonic inhibition (Ataka & Gu, 2006). Layer V neurons from IP3R2KO mice exhibited a lower frequency of mIPSCs (IP3R2WT: 1.35 ± 0.12 Hz; IP3R2KO: 0.79 ± 0.16 Hz, $n = 5$–6, unpaired t test Student: $p = .02$) with no significant alterations in amplitude (IP3R2WT: 25.35 ± 1.49 pA; IP3R2KO: 28.82 ± 7.41 pA, $n = 5$–6, unpaired t test Student: $p = .63$), rise (IP3R2WT: 4.37 ± 0.20 ms; IP3R2KO: 4.17 ± 0.30 ms, $n = 5$–6, unpaired t test Student: $p = .59$) or decay (IP3R2WT: 29.17 ± 0.95 ms; IP3R2KO: 28.97 ± 0.94 ms, $n = 5$–6, unpaired t test Student: $p = .88$, Figure S3C). Considering that changes in mIPSC amplitude are indicative of postsynaptic alterations, while mIPSC frequency changes are indicative of altered presynaptic function or synapse number, our findings suggest that the disruption of proper Ca^{2+} signaling in astrocytes leads to an impairment of presynaptic GABA release.

Astrocytic CB1R signaling role in mPFC information coding is poorly understood. The annulment of CB1R-mediated Ca^{2+} transients in these mice has been reported in several papers (Baraibar et al., 2023; Gómez-Gonzalo et al., 2015; Martín et al., 2015; Martin-Fernandez et al., 2017). To confirm the absence of CB1R-mediated responses of astrocytes of IP3R2KO mice, _ex vivo_ Ca^{2+} experiments were performed in layer V astrocytes in the mPFC of IP3R2WT and IP3R2KO mice (Figure 4a). Indeed, application of a WIN-55212-2 (WIN), a CB1R agonist used in _ex vivo_ Ca^{2+} imaging to study CB1R responses in astrocytes increased Ca^{2+} event frequency (IP3R2WT$_{basal}$: 0.038 ± 0.02 min^{-1}; IP3R2WT$_{WIN}$: 0.14 ± 0.02 min^{-1}, $n = 114$ ROIs from five animals, Holm-corrected Welch's t test: $p < .05$) and event amplitude (IP3R2WT$_{basal}$: 0.00029 ± 0.00012 ΔF/F$_0$; IP3R2WT$_{WIN}$: 0.0015 ± 0.0002 ΔF/F$_0$, $n = 114$ ROIs from five animals, Holm-corrected Welch's t test: $p < .05$, Figure 4b–e) in wild-type mice. Contrarily, in IP3R2KO mice, WIN failed to elicit any changes in frequency (IP3R2W.T$_{basal}$: 0.038 ± 0.02 min^{-1}; IP3R2WT$_{WIN}$: 0.14 ± 0.02 min^{-1}, $n = 114$ ROIs from five animals, Holm-corrected Welch's t test: $p < .05$), amplitude or duration with values basically registering as null (Figure 4b–f). Therefore, IP3R2KO mouse emerges as a highly relevant model to investigate astrocytic CB1R-mediated Ca^{2+} signaling since astroglial CB1R activation elicits Ca^{2+} elevations (Navarrete & Araque, 2008; Robin et al., 2018), the comparison between the responses in IP3R2KO mice with those in the WT littermates (IP3R2WT), allows to highlight the astrocytic CB1R impact upon synaptic plasticity in mPFC.

Next, we studied the effect of astroglial CB1R modulation upon LTP in the mPFC of IP3R2KO mice. In IP3R2WT mPFC slices, LTP magnitude was significantly increased when CB1R agonist, ACEA (1 μM), was present for at least 20 min prior to LTP induction (IP3R2WT$_{(CTL)}$43.2 ± 9.35%; IP3R2WT$_{(ACEA)}$: 115.08 ± 13.81%, $n = 4$–7, one-way ANOVA: $F_{(3,17)} = 12.17$, $p = .0011$, Figure 4g1–g3). This effect corresponds to a significant potentiation of the LTP magnitude by CB1R activation since the effect of ACEA incubation upon LTP was lost in the presence of CB1R antagonist AM251 (1 μM) (IP3R2WT$_{(ACEA)}$: 115.08 ± 13.81%; IP3R2WT$_{(AM251-ACEA)}$: 64.33 ± 17.25, $n = 4$, one-way ANOVA: $F_{(3,17)} = 12.17$, $p = .043$, Figure 4g1–g3). Bath application of AM251 alone did not significantly affect LTP magnitude (IP3R2WT$_{(CTL)}$: 43.2 ± 9.35%; IP3R2WT$_{(AM251)}$: 22.67% ± 4.96, $n = 5$–7, one-way ANOVA: $F_{(3,17)} = 12.17$, $p = .46$, Figure 4g1–g3). Notably, in IP3R2KO slices, that lack astrocytic Ca^{2+}

signaling, ACEA bath application induced a significant decrease of LTP magnitude (IP3R2KO$_{(CTR)}$: 93.85 ± 7.86%; IP3R2KO$_{(ACEA)}$: 29.81 ± 7.38%, one-way ANOVA: $F_{(3,20)} = 8.90$, $p = .0004$, $n = 5$, Figure 4h1–h3). Incubation of IP3R2KO slices with AM251, as well as AM251 plus ACEA, did not elicit any significant changes in LTP magnitude when compared to naïve slices (IP3R2KO$_{(AM251)}$: 65.19 ± 12.58%; IP3R2KO$_{(AM251+ACEA)}$: 56.01 ± 5.86%, one-way ANOVA: $F_{(3,20)} = 8.90$, $p = .0004$, $n = 5$), (Figure 4h1–h3). These results show that CB1R activation has an opposite effect on synaptic plasticity in the mPFC depending on the occurrence of astrocytic Ca^{2+} signaling. It is worth noting that the CB1R agonist under conditions of smaller LTP magnitude (Ca^{2+} signaling present in astrocytes) has a clear facilitatory effect while in the absence of astrocytic Ca^{2+} signaling, and subsequent exacerbated LTP magnitude, its effect is evidently inhibitory, thus suggesting an homeostatic role of these receptors upon LTP.

2.4 | Astrocytic Ca^{2+}-signaling is required for the A_1R-mediated control of CB1R effect upon LTP in the mPFC

During HFS events increased amounts of ATP are released (Cunha, Correia-de-Sá, et al., 1996), originating increased levels of adenosine that will activate adenosine receptors which can have a modulatory action upon CB1R (Hoffman et al., 2010; Sousa et al., 2011). Since we observed that A_1R activation can potentiate CB1R-mediated Ca^{2+} transients in cultured astrocytes, we aimed at testing if the mPFC LTP potentiation by CB1R is also under the control of A_1R. LTP was thus induced in mPFC in the presence of the A_1R antagonist, DPCPX (50 nM), and CB1R agonist, ACEA (1 μM). In IP3R2WT slices DPCPX, applied 30 min before LTP induction, did not significantly affect LTP magnitude (IP3R2WT$_{(CTR)}$: 38.99 ± 9.11%, IP3R2WT$_{(DPCPX)}$: 40.04 ± 13.41%, $n = 8$, one-way ANOVA: $F_{(3,20)} = 9.57$, $p = .99$, Figure 5a1–a3). However, when IP3R2WT slices were superfused with DPCPX prior to ACEA, the A_1R antagonist abolished the ACEA potentiation of LTP (IP3R2WT$_{(ACEA)}$: 106.7 ± 13.62%, IP3R2WT$_{(DCPX+ACEA)}$: 43.04 ± 13.41%, $n = 5$–8, one-way ANOVA: $F_{(3,20)} = 9.57$, $p = .003$, Figure 5a1–a3). These results suggest that in the presence of astrocytic Ca^{2+} signaling, CB1R potentiation of LTP in mPFC is under the control of A_1R. Notably, in mPFC slices of IP3R2KO, ACEA was still able to inhibit LTP despite the presence of DPCPX (IP3R2KO$_{(ACEA)}$: 27.18 ± 10.06%, IP3R2KO$_{(DPCPX+ACEA)}$: 35.82 ± 16.13%, $n = 4$, one-way ANOVA: $F_{(3,12)} = 6.50$, $p = 0.97$, Figure 5b1–b3). Altogether, the results show that A_1R is necessary for the influence of CB1R in mPFC LTP but that this action requires astrocytic Ca^{2+} signaling.

2.5 | The absence of astrocytic Ca^{2+} signaling unmasks a facilitatory action of $A_{2A}R$ in mPFC synaptic plasticity, but $A_{2A}R$ blockade does not affect the action of CB1R in mPFC LTP

Our finding that $A_{2A}R$ decreases CB1R-mediated Ca^{2+} signaling in astrocytes in situ, prompted the hypothesis that $A_{2A}R$ could

downregulate CB1R potentiation of LTP magnitude. To test this hypothesis, LTP was induced in the presence of the $A_{2A}R$ antagonist, SCH58261 (50 nM), and the CB1R agonist ACEA (1 μM). In IP3R2WT

slices, SCH58261 bath application resulted in an LTP magnitude that was not significantly different from the LTP magnitude of the control condition, without any drug added (IP3R2WT$_{(CTR)}$: 35.37 ± 7.75%;
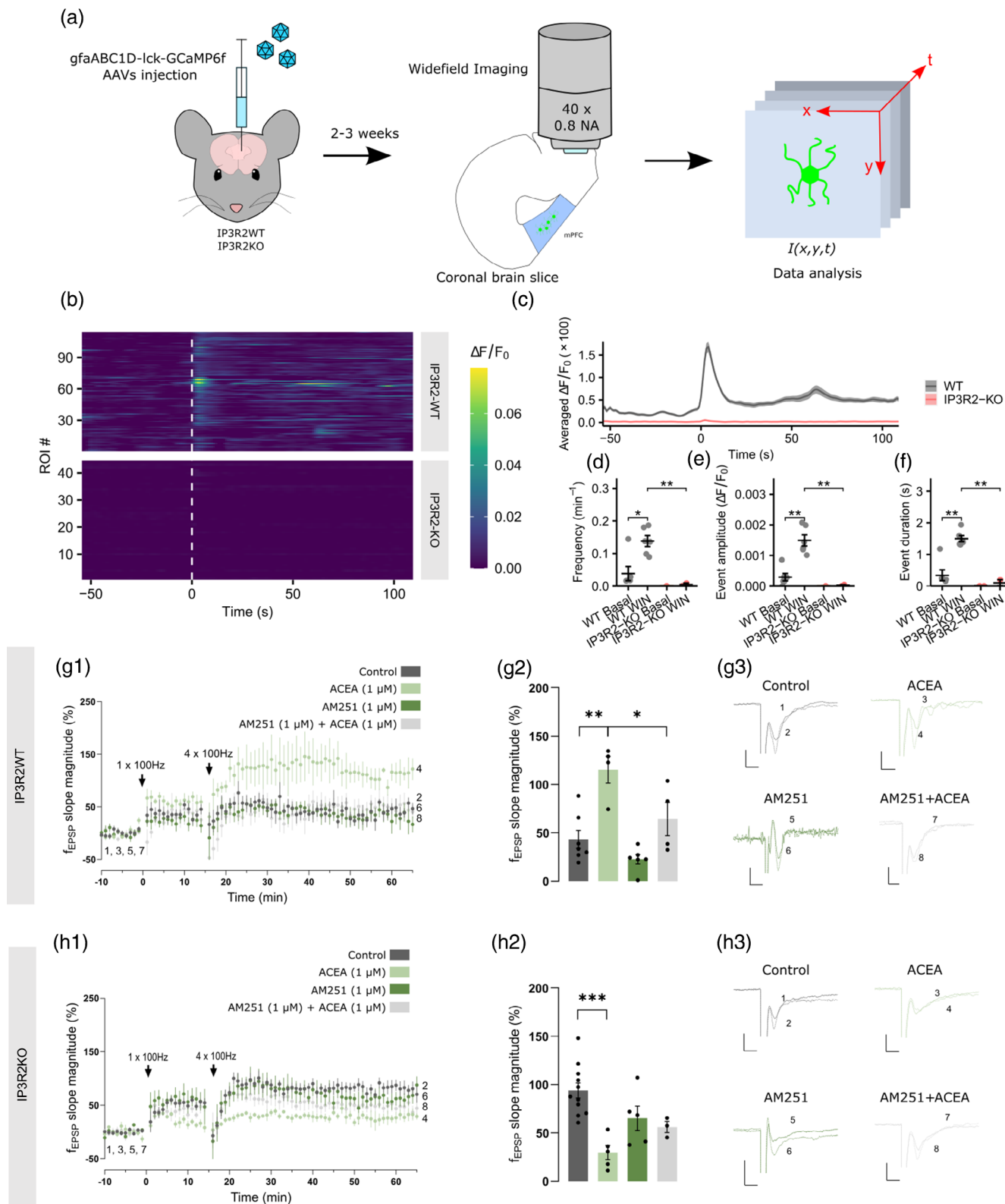

FIGURE 4 Legend on next page.

IP3R2WT$_{(SCH58261)}$: 53.93 ± 14.44%, $n = 4$–10, one-way ANOVA: $F_{(3,20)} = 6.82$, $p = .79$, Figure 6a1–a3). Unlike what we observed for A$_1$R when IP3R2WT brain slices were superfused with SCH58261 prior to ACEA, CB1R enhancement of LTP magnitude was not lost (IP3R2WT$_{(ACEA)}$: 106.7 ± 13.62%, IP3R2WT$_{(SCH58261+ACEA)}$: 98.82 ± 23.96%, $n = 4$–5, one-way ANOVA: $p = .98$, Figure 6a1–a3), suggesting that the antagonism of A$_{2A}$R does not affect CB1R-mediated potentiation of LTP in mPFC. In this new series of experiments, the inhibition of LTP caused by ACEA in IP3R2KO slices was evident as before (IP3R2KO$_{(CTR)}$: 96.31 ± 11.37%; IP3R2KO$_{(ACEA)}$: 27.19 ± 10.06%, $n = 4$–6, one-way ANOVA: $F_{(3,14)} = 6.63$, $p = .023$). Interestingly SCH58261 also caused a significant inhibition of LTP (IP3R2KO$_{(CTR)}$: 96.31 ± 11.37%; IP3R2KO$_{(SCH58261)}$: 17.46 ± 20.79%, $n = 4$–6, one-way ANOVA: $F_{(3,14)} = 6.63$, $p = .0094$, Figure 6b1–b3), suggesting that in the absence of astrocytic Ca^{2+}-signaling a tonic A$_{2A}$R-mediated facilitatory action is unmasked. In IP3R2KO, the presence of SCH58261 did, however, not affect the inhibitory action of ACEA upon LTP magnitude (IP3R2KO$_{(ACEA)}$: 27.19 ± 10.06%, IP3R2-KO$_{(ACEA+SCH58261)}$: 30.89 ± 18.88, $n = 4$, one-way ANOVA: $F_{(3,14)} = 6.63$, $p = .99$, Figure 6b1–b3), suggesting that A$_{2A}$R does not affect the CB1R effect on mPFC synaptic plasticity in the absence of astrocytic Ca^{2+} signaling.

3 | DISCUSSION

The main finding of this work is the identification of a functional crosstalk between A$_1$R-CB1R and A$_{2A}$R-CB1R heteromers in cortical astrocytes, where ADOR can modulate CB1R-mediated Ca^{2+} signaling. Furthermore, we show that LTP in mPFC is higher in the absence of astrocytic Ca^{2+} signaling (IP3R2KO mice) and that this exacerbated LTP requires activation of adenosine A$_{2A}$R by endogenous adenosine. Remarkably, CB1R activation has a dual influence upon mPFC LTP: a facilitatory action that requires A$_1$R co-activation and astrocytic Ca^{2+} signaling, and an inhibitory action independent of A$_1$R (see Figure 7).

3.1 | ADOR-CB1R heteromers are present in astrocytes

We detected exogenous and endogenous A$_1$R-CB1R and A$_{2A}$R-CB1R heteromers, in astrocytes. Importantly, we discovered that the heteromerization of CB1R with both adenosine A$_1$ and A$_{2A}$ receptors depends on the levels of extracellular adenosine since PLA assays unveiled a significant decrease of A$_1$R-CB1R heteromer and a significant increase of A$_{2A}$R-CB1R heteromer when extracellular adenosine was removed. This is probably because adenosine receptor heteromers act as adenosine sensors, regulating cell activity homeostatically (Ciruela et al., 2006; Cristóvão-Ferreira et al., 2013). Indeed, adenosine has a higher affinity to A$_1$R (Borea et al., 2018), thus at low adenosine concentrations A$_1$R is preferably activated in neurons and astrocytes (Cristóvão-Ferreira et al., 2013; Köfalvi et al., 2020). In contrast, moderately higher concentrations also activate A$_{2A}$R, antagonizing A$_1$R function in neurons and astrocytes (Cristóvão-Ferreira et al., 2013; Köfalvi et al., 2020; Marchi et al., 2002). Notably, our work shows the first crosstalk between these receptors in astrocytes, and to our knowledge the first reported existence of A$_1$R-CB1R.

3.2 | Astrocytic CB1R-Ca^{2+} signaling is influenced by adenosine receptors

Given the relevance of heteromers in Ca^{2+} signaling (e.g. D1R-D2R heteromers), we explored the potential role of ADOR-CB1R heteromers on CB1R-mediated Ca^{2+} signaling. To start, we evaluated the role of endogenous adenosine. To our surprise, extracellular adenosine removal under our culture conditions did not lead to significant alterations in CB1R-Ca^{2+} signaling. Given that CB1R-signaling was affected by exogenous activation of ADOR, this may result from the washing out of extracellular adenosine to levels below the threshold required to activate ADOR, rather than from the absence of influence of ADOR upon the action of CB1R since CB1R-signaling was clearly affected by exogenous activation of ADOR. Adenosine A$_{2A}$R can

FIGURE 4 CB1R activation has a dual effect on mPFC II/III-V synapse LTP. (a) Wild-type (WT) and IP3R2KO mice were injected with gfaABC1D-lck-GCaMP6f-expressing AAVs in the medial prefrontal cortex. GCaMP6f fluorescence was imaged in acute slices before and after a 3-s puff of 300 μM WIN-55212–2. (b) Heatmap of the GCaMP6f fluorescence signal in WT and IP3R2KO astrocytes. (c) Averaged ΔF/F0 fluorescence trace in WT and IP3R2-KO astrocytes. Ca^{2+} event frequency (d), amplitude (e) and duration (f) before (Basal) and after WIN averaged per slice. Data are presented as mean ± SEM of 44–114 ROIs from 2 to 6 slices, $n = 1$–5 animals per genotype, *$p < .05$, **$p < .01$ assessed by Holm-corrected Welch's *t* test. Time course of CB1R-mediate effect on the mPFC layer V LTP in brain slices from IP3R2WT (g1) and IP3R2KO mice (g1): in control condition (black), with bath application of ACEA (1 μM) for 20 min before LTP induction (light green), with bath application of AM251 (1 μM) 30 min prior to LTP induction (dark green) and with bath application of AM251 for 30 min before bath application of ACEA 20 min prior to LTP induction (light gray). Comparison of LTP magnitudes for the IP3R2WT (g1) and IP3R2KO (h1) mice obtained in the experiments illustrated in (g2) and (h2) (see methods for further details). Representative traces of fEPSPs (preceded by the stimulus artifact and the pre-synaptic volley) recorded before (1, 3, 5, and 7, dashed line) and after (2, 4, 6, and 8, continuous line) inducing LTP in slices from IP2R2WT (g3) and IP3R2KO (h3) mice, under the different condition: control condition (1 and 2, black), ACEA (1 μM) (3 and 4, light green), AM251 (1 μM) (5 and 6, dark green) and AM251 together with ACEA (7 and 8, light gray); tracings recorded from the same slice are superimposed. For IP3R2WT mice experiments: data are mean ± SEM of 4–7 slices from different animals per condition. *$p < .05$, **$p < .01$ assessed by one-way A-NOVA followed by Bonferroni correction. For IP3R2KO mice experiments: data are mean ± SEM of 3–11 slices per condition. ***$p < .001$ assessed by one-way A-NOVA followed by Bonferroni correction. Scale of representative traces: 0.5 mV, 5 ms.
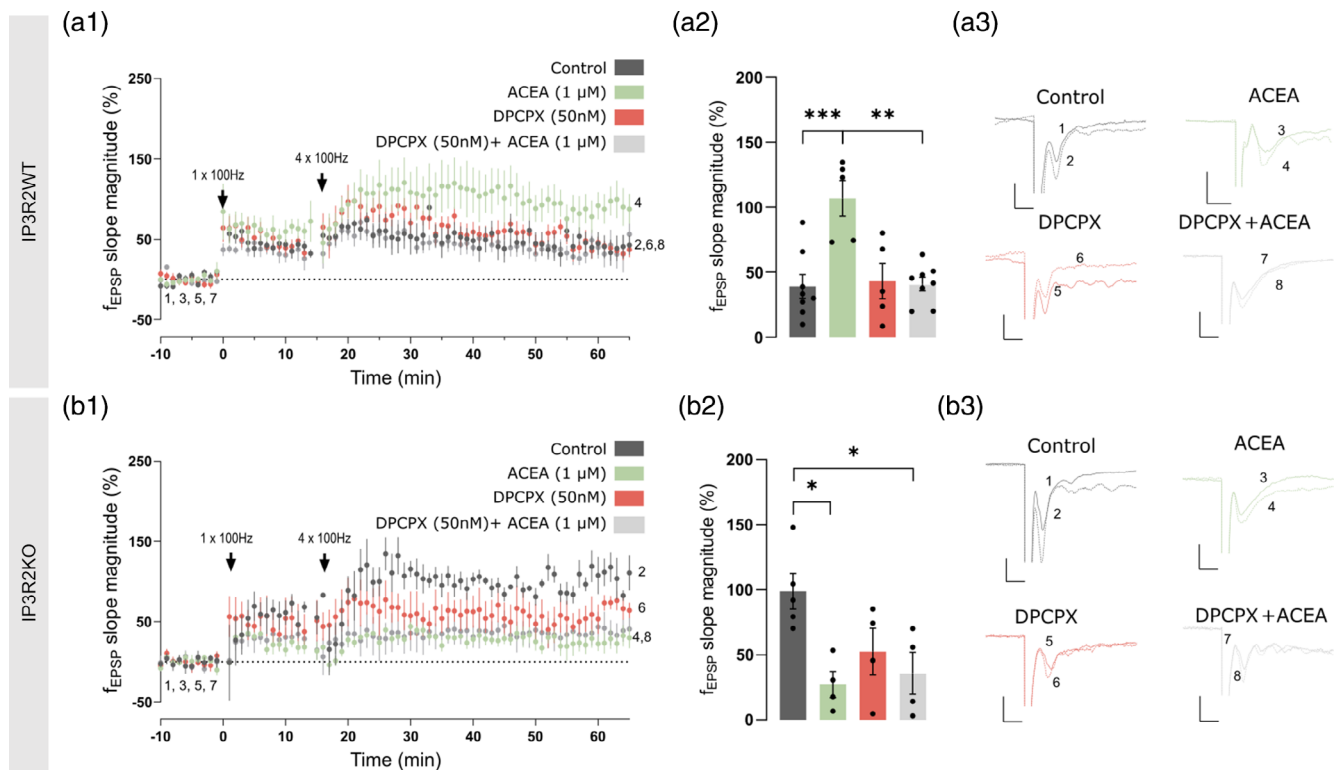
FIGURE 5 The CB1R effect on mPFC LTP in IP3R2WT mice is A1R-dependent. Time course of CB1R-mediate effect on the mPFC layer V LTP in brain slices from IP3R2WT (a1) and IP3R2KO mice (b1): in control condition (black), with bath application of ACEA (1 μM) for 20 min before LTP induction (light green), with bath application of DPCPX (50 nM) 30 min prior to LTP induction (red) and with bath application of DPCPX for 30 min before bath application of ACEA 20 min prior to LTP induction (light gray). Comparison of LTP magnitudes for the IP3R2WT (A2) and IP3R2KO (b2) mice obtained in the experiments illustrated in (a1) and (b1), respectively (see methods for further details). Representative traces of fEPSPs (preceded by the stimulus artifact) recorded before (1, 3, 5, and 7, dashed line) and after (2, 4, 6, and 8, continuous line) inducing LTP in slices from IP2R2WT (a3) and IP3R2KO (b3) mice, under different condition: control condition (1 and 2, black), ACEA (1 μM) (3 and 4, light green), DPCPX (50 nM) (5 and 6, red) and DPCPX together with ACEA (7 and 8, light gray); tracings recorded from the same slice are superimposed. Data are mean ± SEM of 5–8 slices from different animals per condition. $*p < .05$, $**p < .01$, $***p < .001$ assessed by one-way A-NOVA followed by Bonferroni correction. Scale bar of representative traces: 0.5 mV, 5 ms.

facilitate the activity of adenosine transporters (Delicado et al., 1990; Pinto-Duarte et al., 2005) thus ADA was added to the medium while testing the action of ADOR agonists. Our findings revealed that A_1R activation facilitates CB1R-mediated Ca^{2+} signaling, while $A_{2A}R$ decreased it. This highlights that ADORs act as the switch for CB1R-Ca^{2+} signaling. Although previous studies have demonstrated hetero-merization between $A_{2A}R$ and CB1R, as well as the inhibitory effect of $A_{2A}R$ activation on CB1R signaling (Chiodi et al., 2016; Ferreira et al., 2015; Köfalvi et al., 2020) (Chiodi et al., 2016; Ferreira et al., 2015) our study is the first to observe these interactions in astrocytes and its intrinsic Ca^{2+} signaling.

Furthermore, our data extend these interactions to A_1R, and the dual role that extracellular adenosine may have, facilitating or inhibiting CB1R signaling depending on the activated ADOR. Since the type of activated ADOR may depend on the level of neuronal and astrocytic activity (Agostinho et al., 2020; Covelo & Araque, 2018; Köfalvi et al., 2020), altogether our data suggests that the heteromerization between CB1R and ADOR in astrocytes contributes to the homeostatic control of astrocytic Ca^{2+} signaling. In turn, this likely plays a crucial role in the control of astrocyte-to-neuron signaling. Indeed, at low levels of activity, A_1R is

predominantly activated (Ciruela et al., 2006; Cristóvão-Ferreira et al., 2013), facilitating CB1R-mediated Ca^{2+} signaling, whereas, at higher levels of activity, $A_{2A}R$ activation prevails, inhibiting CB1R-Ca^{2+} signaling.

3.3 | IP3R2KO model is suitable to study astrocytic CB1R activation

Astrocytic CB1R-mediated Ca^{2+} signaling is relevant in synaptic plasticity in various brain regions (Baraibar et al., 2023; Gómez-Gonzalo et al., 2015; Han et al., 2012; Martin-Fernandez et al., 2017). Thus, we aimed to study its role upon synaptic plasticity in the mPFC, which is associated with executive functions and emotional behavior (Simpson et al., 2001; Smith et al., 2018). While caffeine (an adenosine analog) and cannabinoids are known to affect this area, their impact is predominantly attributed to neuronal receptors. It is crucial to discern the specific effects mediated by astrocytic receptors to understand potential distinct outcomes. Thus, we used the IP3R2KO mouse model (Li et al., 2005) with a constitutive gene deletion, as a valuable genetic tool to study IP3R-dependent Ca^{2+} signals in astrocytes processes and soma
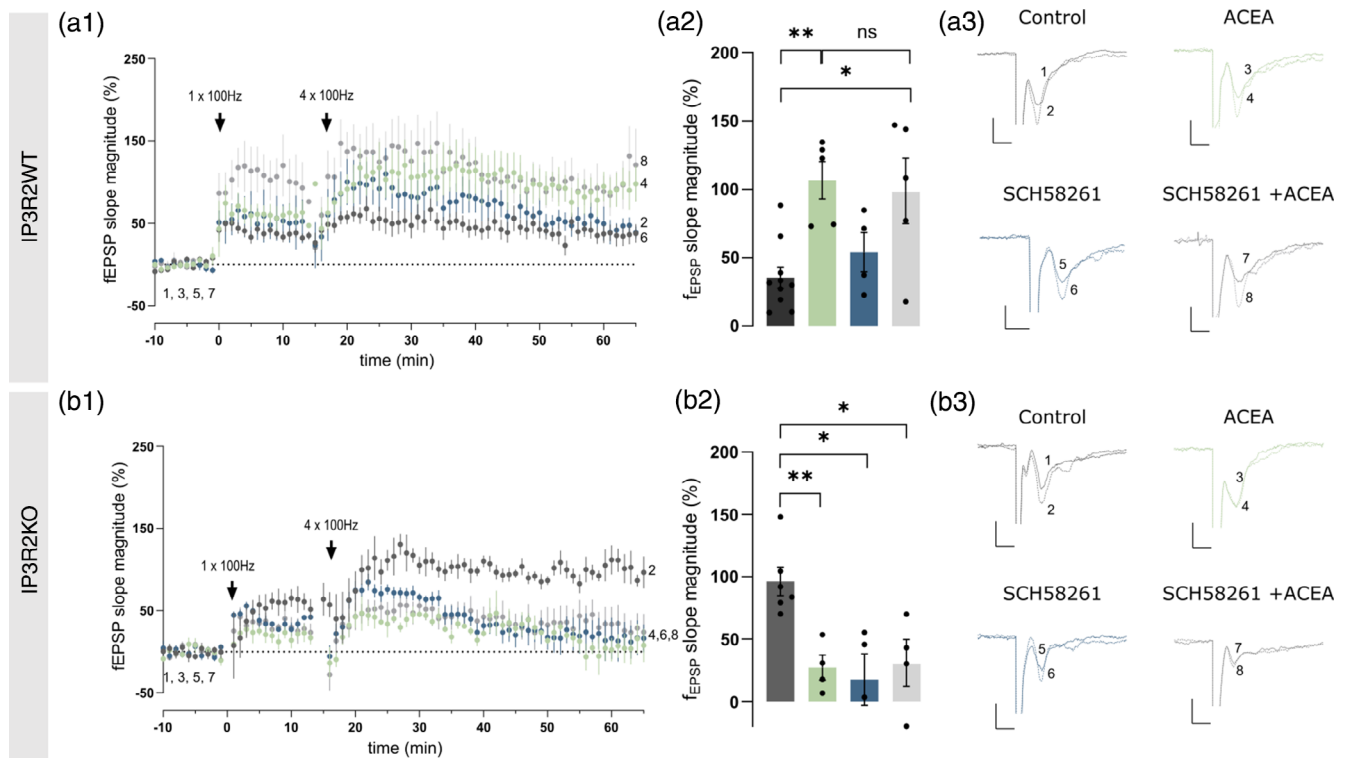
FIGURE 6 The CB1R effect on mPFC LTP is not modulated by $A_{2A}R$. Time course of CB1R-mediate effect on the mPFC layer V LTP in brain slices from IP3R2WT (a1) and IP3R2KO mice (b1): in the control condition (black), with bath application of ACEA (1 μM) for 20 min before LTP induction (light green), with bath application of Scheme (50 nM) 30 min before LTP induction (blue) and with bath application of DPCPX for 30 min before bath application of ACEA 20 min before LTP induction (light gray). Comparison of LTP magnitudes for the IP3R2WT (a2) and IP3R2KO (b2) mice obtained in the experiments illustrated in (a1) and (a1), respectively (see methods for further details). Representative traces of fEPSPs (preceded by the stimulus artifact) recorded before (1, 3, 5, and 7, dashed line) and after (2, 4, 6, and 8, continuous line) inducing LTP in slices from IP2R2WT (a3) and IP3R2KO (b3) mice, under the different condition: control condition (1 and 2, black), ACEA (1 μM) (3 and 4, light green), purple (50 nM) (5 and 6, blue) and DPCPX together with ACEA (7 and 8, light gray); tracings recorded from the same slice are superimposed. Data are mean ± SEM of 3–7 slices from different animals per condition. *$p < .05$, **$p < .01$ assessed by one-way A-NOVA followed by Bonferroni correction. Scale of representative traces: 0.5 mV, 5 ms.

(Agulhon et al., 2010; Di Castro et al., 2011; Guerra-Gomes et al., 2020; Navarrete et al., 2012; Panatier et al., 2011; Petravicz et al., 2008). Before proceeding with the main experiments, we sought to unveil the impact of IP3R2-signaling on synaptic plasticity in the mPFC, specifically LTP. A stronger LTP was revealed in IP3R2KO compared with IP3R2WT mice. This observation could potentially be attributed to the absence of astrocytic GABA release. Astrocytes are able to release the inhibitory neurotransmitter GABA in a Ca^{2+}-dependent manner (Lee et al., 2010), leading to tonic inhibition of various neuronal circuits (Goenaga et al., 2023). Thus, the removal of this tonic inhibition in the IP3R2KO mice might contribute to the increased LTP. To confirm this, mIPSCs were measured in layer V neurons, revealing a lower frequency in IP3R2KO, aligning with reduced tonic inhibition, corroborating our hypothesis. However, further studies are needed to validate this hypothesis. Another possibility underlying this effect is that in IP3R2KO mice, parvalbumin interneuron depolarization fails to enhance inhibitory synaptic transmission due to compromised astrocyte ATP/adenosine release (Mederos et al., 2021) increasing LTP. Indeed, the absence of ATP/adenosine from astrocytes could contribute to the loss of adenosine A1 tonic activation, which, as indicated by our results, may account for the increased magnitude of LTP.

Nevertheless, both genotypes presented a stable LTP by HFS, establishing IP3R2KO mice as a robust model to study LTP in the rodent mPFC. Beyond this, it was reassured that astrocytic CB1R-mediated Ca^{2+} signaling was absent in IP3R2KO. Ex vivo Ca^{2+} imaging experiments in layer V astrocytes of the mPFC demonstrated that WIN 55,212-2, a synthetic cannabinoid used in this type of experiments, increased Ca^{2+} events while failing to do so in IP3R2KO, in line with other brain regions (Navarrete & Araque, 2008; Oliveira da Cruz et al., 2016; Robin et al., 2018). Thus, this model emerges as a good model to evaluate the role of astroglial CB1R on synaptic plasticity. In the absence of astrocytic Ca^{2+} signaling, any action of CB1 receptor ligand in IP3R2KO mice is unlikely resulting from an action of astrocytic CB1R.

3.4 | CB1R activation has a dual effect on LTP depending on proper astrocytic Ca^{2+} signaling

Astrocytes play a key role in the functioning of mPFC (Banasr & Duman, 2008; Brockett et al., 2018; Lima et al., 2014; Mederos et al., 2021), however, the role of astrocytic CB1R on synaptic

FIGURE 7 Schematic representation of the mechanism of mPFC LTP modulation by astrocytic CB1R-A_1R heteromers. Under physiological astrocytic Ca^{2+} levels, in IP3R2WT mice (linear black arrows), CB1R potentiates mPFC LTP requiring A_1R co-activation (linear *fEPSPs*). In the absence of astrocytic Ca^{2+} signaling, in IP3R2KO mice, mPFC LTP is higher (dashed *fEPSPs*) and requires activation of adenosine A_{2A}R by endogenous adenosine (dashed inhibition arrow). Moreover in the absence of astrocytic Ca^{2+} signaling LTP is inhibited by CB1R activation independently of A_1R (red dashed inhibition arrows).
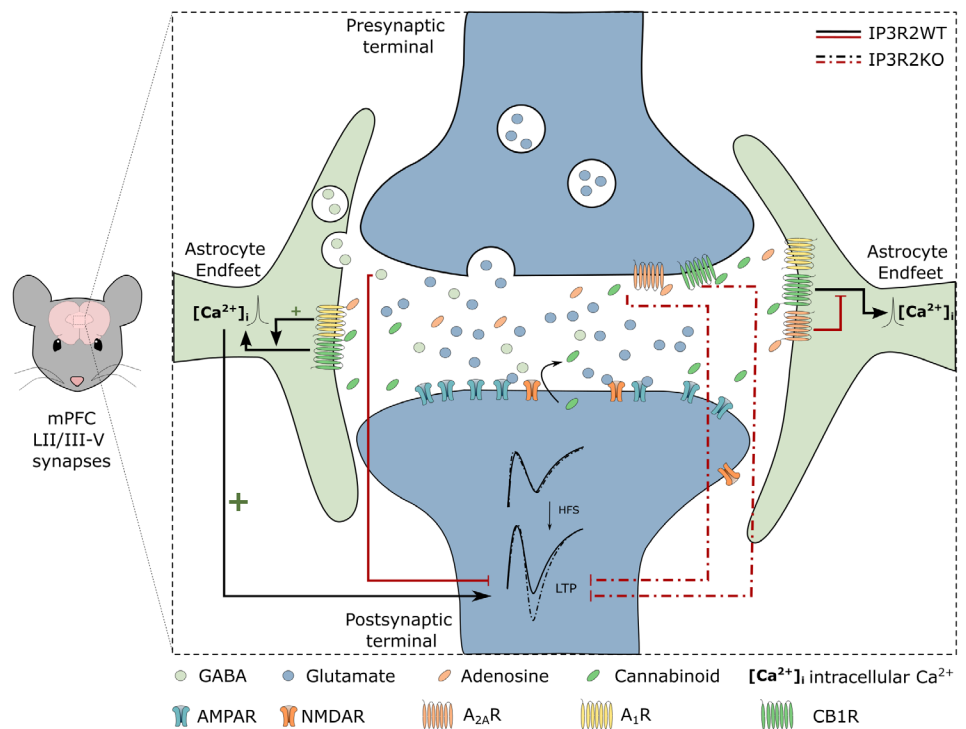
plasticity in this brain area was unknown. Thus, we investigated the role of astrocytic CB1R activation in mPFC LTP. CB1R activation potentiated mPFC LTP in the IP3R2WT mice, while decreasing it in IP3R2KO mice. Both effects were confirmed to be mediated by CB1R, since they were abolished in the presence of a selective CB1R antagonist. Overall, the results present the dual role of CB1R in synaptic plasticity in the mPFC highlighting the dependence of astrocytic Ca^{2+} signal, thus providing a novel key role for the astrocytic CB1R.

Previous studies report that hippocampal CB1R modulation has a dual role in θ-burst-induced CA1 LTP magnitude based on the strength of LTP induction and on the nature of CB1R activators (Silva-Cruz et al., 2017). However, this duality is independent of astrocyte activity, at least in LTP induced by strong θ-burst stimulation. Furthermore, hippocampal CB1R activation facilitates LTP induced by a strong θ-burst stimulation and inhibits LTP induced by a weak θ-burst stimulation, a contrast to our findings in the mPFC.

Our study reveals that in the mPFC, CB1R may function as homeostatic regulators of plasticity, rather than acting as a high-pass filter of synaptic plasticity as suggested for the hippocampus (Silva-Cruz et al., 2017). Usually, CB1R activation pathways in the brain network have inhibitory consequences (Basavarajappa et al., 2014; Bohme et al., 1999), and eCB signaling upon synaptic plasticity is mainly associated with synaptic depression (Han et al., 2012). However, our study demonstrates that CB1R activation potentiates LTP magnitude in the mPFC in IP3R2WT mice, challenging the conventional view. Supporting our hypothesis that astrocytes and consequently astrocytic CB1R are crucial participants in LTP, not only the facilatory effect of CB1R was lost but is reversed in the mPFC of IP3R2KO mice. This observation emphasizes the contribution of astrocytes and astrocytic CB1R as fundamental players in triggering LTP. Further corroborating our

hypothesis is the well-established evidence that *in vivo* hippocampal LTP, induced by HFS, and heterosynaptic potentiation at excitatory hippocampal CA3-CA1 synapses are both dependent on astrocytic CB1R (Navarrete & Araque, 2010; Robin et al., 2018). Moreover, eCBs can trigger LTP through stimulation of astrocyte–neuron signaling (Gómez-Gonzalo et al., 2015), these observations being in accordance with our data. This highly suggests that in the absence of Ca^{2+} signaling in astrocytes, CB1R agonists will mainly activate neuronal CB1R which are known to be inhibitory by decreasing the neurotransmitter release (Chevaleyre et al., 2006), ultimately leading to a decrease in LTP magnitude. In contrast, when the astrocytic Ca^{2+} signaling was intact the influence of CB1R upon the astrocytes likely prevails, the consequent increase in intracellular Ca^{2+} levels leads to the release of a yet unknown gliotransmitter that facilitates LTP. Thus, astrocytic CB1R enhancement of LTP is most likely regulated by astrocytic Ca^{2+} signaling, as this effect is lost in IP3R2KO mice.

3.5 | CB1R-mediated LTP potentiation is under A_1R control

Astrocytes and neurons release ATP (Agostinho et al., 2020) which is rapidly converted to adenosine activating A_1R or A_{2A}R, regulating synaptic transmission and plasticity (Baraibar et al., 2023; Fredholm et al., 2005; Gonçalves et al., 2023; Lalo et al., 2014; Pascual et al., 2005). Adenosine also modulates the functionality of other receptors including the CB1R (Mouro et al., 2017, 2019; Silva-Cruz et al., 2017; Sousa et al., 2013), as previously mentioned.

Considering that our study reported adenosine receptors as modulators of CB1R-mediated Ca^{2+} signaling, we hypothesized that this

modulation could impact the mPFC synaptic plasticity in the mPFC. To study the role of ADOR modulation upon the astrocytic CB1R-mediated effect on LTP in the mPFC, we selectively blocked either A_1R or the $A_{2A}R$ while activating CB1R using the IP3R2KO mouse model. Importantly, we abstained from enzymatically removing endogenous adenosine in this set of experiments to avoid potential epileptiform activity, as adenosine deficiency is a hallmark of epilepsy (Boison, 2008, 2016).

In mPFC slices from IP3R2WT mice, the blockade of A_1R did not change LTP magnitude. However, when CB1R was activated while blocking the A_1R, the CB1R-mediated LTP potentiation was lost. Notably, in the IP3R2KO mPFC slices, the A_1R blockade did not appreciably affect the inhibitory action of CB1R upon LTP. This is in accordance with data from other brain regions, where LTP induced by HFS is not affected by knocking out the A_1R gene (Giménez-Llort et al., 2005). Our findings that in the absence of functional astrocytic Ca^{2+} signaling the activity of A_1R over the action of CB1R upon LTP is lost, coupled with the evidence for the heteromerization of A_1R with CB1R in astrocytes, suggest the necessity of A_1R-CB1R heteromers in fully functional astrocytes for a proper potentiation of LTP magnitude by CB1R. This is supported by the observation that CB1R-A1R heteromers are preferentially formed in the presence of endogenous adenosine and the activation of A_1R potentiated the CB1R-mediated Ca^{2+} in astrocytes. The collective findings reinforce the role of astrocytic heteromers in orchestrating the potentiation of LTP by CB1R.

Moreover, astrocytic ATP release is mostly associated with A_1R activation, regulating basal synaptic transmission (Fredholm et al., 2005). Synaptic ATP release is more prominent at higher frequencies (Cunha, Vizi, et al., 1996; Wieraszko et al., 1989) that are associated with synaptic plasticity processes involved in learning and adaptive processes and predominantly activating $A_{2A}R$ rather than A_1R (Cunha, Correia-de-Sá, et al., 1996). This astrocytic Ca^{2+} potentiation can enhance gliotransmitter release, potentially impacting synaptic plasticity. If the gliotransmitter involved is ATP, mostly associated with A_1R activation (Corkrum et al., 2020; Covelo & Araque, 2018), the CB1R effect can be further potentiated. The observation that A_1R does not affect CB1R action upon LTP in the absence of astrocytic Ca^{2+} signaling suggests that the interplay between A_1R and CB1R to modulate LTP occurs in astrocytes. Since both neuronal CB1R and A_1R are Gi/o protein-coupled receptors, it is likely that in neurons, both receptors are mediating their effects through the same signaling pathway, both contributing to a decrease in LTP magnitude. Further experiments must be performed to address this hypothesis.

3.6 | $A_{2A}R$ blockade does not influence CB1R effect in LTP regardless of astrocytic Ca^{2+} signaling

$A_{2A}R$ blockade did not alter CB1R-mediated effect in LTP both in the IP3R2WT and the IP3R2KO slices. Even though this is not in accordance with previous data (Kerkhofs et al., 2018), it was also reported

in the same study that $A_{2A}R$ blockade did not affect glutamatergic synapse LTP in layer V pyramidal neurons. Considering that the removal of extracellular adenosine increased $A_{2A}R$-CB1R heteromers, we can ponder that under physiological levels of extracellular adenosine, $A_{2A}R$-CB1R heteromer quantity is not sufficient for $A_{2A}R$ to influence the CB1R signaling pathway. Notably, our results suggest that under physiological levels of extracellular adenosine, CB1R primary heteromerizes with A_1R over $A_{2A}R$, since only A_1R modulates CB1R-mediated effect on mPFC LTP in IP3R2WT and the depletion of endogenous adenosine in astrocytic primary cultures decreased A_1R-CB1R and increased $A_{2A}R$-CB1R heteromers. In IP3R2KO mPFC slices, $A_{2A}R$ blockade decreased LTP magnitude. In this condition, Ca^{2+}-dependent gliotransmitter release is compromised, making neurons the main source of adenosine (De Mendonça & Ribeiro, 1994; Düster et al., 2014; Forghani & Krnjević, 1995). We propose that the lack of astrocytic Ca^{2+} signaling and the subsequent compromised gliotransmission result in $A_{2A}R$ overactivation, decreasing LTP magnitude when the receptor is blocked. Thus, CB1R-mediated enhancement of LTP is astroglial Ca^{2+} signaling- and A_1R-dependent while $A_{2A}R$ does not interfere with this effect.

4 | CONCLUSION

In conclusion, this work reports for the first time that the acute activation of CB1R potentiates LTP in the mPFC Layer V in an astrocytic Ca^{2+} signaling-dependent manner, which indicates a pivotal role of the astrocytic CB1R. Furthermore, A_1R modulates this CB1R role upon synaptic plasticity due to the functional CB1-A_1R heteromers identified in astrocytes. It is important to acknowledge that while there are many experimental approaches to explore GPCR heteromers, the majority focus on identification and not direct impact assessment. Thus, while our data can shed light on how CB1R, A_1R, and $A_{2A}R$ receptors influence synaptic function, we cautiously postulate its influence through heteromers without complete assumption of their role. Ultimately, this data can alter how we can approach neurological diseases where the signaling pathways of these receptors are compromised.

5 | METHODS

5.1 | Ethical statement

Animals were maintained in controlled temperature ($21 \pm 1^\circ C$) and humidity ($55 \pm 10\%$) conditions with a 12:12 h light/dark cycle and access to food and water ad libitum. All procedures were carried out according to the European Union Guidelines for Animal Care (European Union Council Directive 2010/63/EU) and Portuguese law (DL 113/2013) with the approval of the Institutional Animal Care and Use Committee. Care was taken to minimize the number of animals sacrificed.

5.2 | Generation of IP3R2-KO mice

A mouse strain with targeted deletion of Itpr2 gene was kindly supplied for this work by Prof. João F. Oliveira (U. Minho, Portugal) (Guerra-Gomes et al., 2020), under agreement with Prof. Ju Chen (U.C. San Diego, USA) (Li et al., 2005), who have generated the IP3R−/− (IP3R2-KO) mice. IP3R2-KO and their respective littermate WT controls were obtained by mating couples of IP3R2+/−. Collected toe tissue was used for DNA extraction and subsequent genotyping by polymerase chain reaction (PCR) analysis using WT (Forward (F), 5′-ACCCTGATGAGGGAAGGTCT-3′; Reverse (R), 5′-ATCGATTCATAGGGCACACC-3′) and mutant allele-specific primers (neo-specific primer: F, 5′-AATGGGCTGACCGCTTCCTC GT-3′; R, 5′-TCTGAGAGTGCCTGGCTTTT-3′) as previously described (Li et al., 2005).

Four to 7 IP3R2WT and 3–11 IP3R2KO were used in the test CB1R effect upon synaptic plasticity. Five to 8 IP3R2WT and 4–5 IP3R2KO were used in the study A1R modulation in CB1R effect upon synaptic plasticity. Four to 10 IP3R2WT and 4–6 IP3R2KO were used in the study A$_{2A}$R modulation in CB1R effect upon synaptic plasticity.

5.3 | Adeno-associated virus injections

Wild-type and IP3R-KO mice were anesthetized with isoflurane (3.5% induction, 1–2% maintenance) and placed in a stereotaxic frame. AAV5 pZac2.1 gfaABC1D-lck-GCaMP6f (Addgene #52924, 2.8×10^{13} gc/mL) was injected (350 nL, 60 nL/min) in the mPFC (M/L: ±0.3, A/P: +1.94, D/V: −3.1). The injection pipette was held in place for 5 min to avoid backflow. Wounds were then sutured and mice were allowed to recover on heating pads until breathing normally and fully awake. Experiments were performed 2–3 weeks after surgery to allow for Adeno-associated virus (AAV) expression.

5.4 | Slice preparation for *ex vivo* Ca^{2+} imaging

mPFC acute slices were prepared from 10 to 14-week-old male and female IP3R2WT and IP3R2KO mice. Briefly, animals were anesthetized with pentobarbital and transcardially perfused with ice-cold recovery solution containing (in mM): N-methyl-D-glucamine 95.3, KCl 2.1, NaH$_2$PO$_4$ 1.2, NaHCO$_3$ 30, HEPES 16.8, Glucose 22.8, Na$^+$ ascorbate 5, thiourea 2, Na$^+$ pyruvate 3, MgSO$_4$ 4.9, CaCl$_2$ 0.5, pH 7.3. The brain was rapidly removed and placed in ice-cold recovery solution for slicing (300 μm) in a Leica VT1200S vibratome. Slices were incubated for <1 min in 34°C recovery solution followed by >1 h incubation in 25°C standard artificial cerebrospinal fluid (ACSF) containing (in mM): NaCl 124, KCl 2.7, KH$_2$PO$_4$ 1.2, MgSO$_4$ 2, NaHCO$_3$ 26, Glucose 9, CaCl$_2$ 2, ascorbic acid 0.4, continuously gassed with 5% CO$_2$/95% O$_2$, pH 7.3.

5.5 | Slice preparation for electrophysiological recordings

Whole brain slices, containing the mPFC, were prepared as previously in our lab (Tanqueiro et al., 2021) from males and females IP3R2-KO mice 8–12 weeks old and the respective age-matched littermates. Animals were sacrificed by decapitation after cervical displacement and the brain was rapidly removed from the skull and dissected in ice-cold dissecting solution containing (in mM): 110 sucrose; 2.5 KCl; 0.5 CaCl$_2$; 7 MgCl$_2$; 25 NaHCO$_3$; 1.25 NaH$_2$PO$_4$; 7 glucose, pH 7.4, and gassed with 95% O$_2$ and 5% CO$_2$. For the electrophysiology recordings in the mPFC, coronal slices (300 μm thick) were cut with a Vibratome (VT 1000S; Leica, Nussloch, Germany). The slices were then transferred to a recover chamber containing aCSF with the following composition (in mM): 124 NaCl, 3 KCl, 1.2 NaH$_2$PO$_4$, 25 NaHCO$_3$, 2 CaCl$_2$, 1 MgSO$_4$, and 10 glucose, pH 7.4, continuously gassed with 95% O$_2$ and 5% CO$_2$. Slices were left to recover for at least 1 h at RT before starting the recording.

5.6 | Primary astrocytic cultures

Primary cortical astrocytes were obtained from 0 to 2 days old Sprague Dawley (Charles River, Barcelona, Spain) pups of either sex as described by Vaz et al., 2011. Pups were sacrificed by decapitation and the heads were sterilized by submersion in 70% ethanol three times. The brains of the pups were dissected in phosphate-buffered saline (PBS, in mM: 137 mM NaCl, 2.7 mM KCl, 8 mM Na$_2$HPO$_4$.2H2O, and 1.5 mM KH$_2$PO$_4$, pH 7.4) out by removing the scalp covering the top part of the skull. A midline incision was made in the skull exposing the brain which was then dissected out by introducing a spatula between the cortex and olfactory bulbs separating them and sliding the spatula under the brain cutting the optical nerves and removing the brain from the skull. The cerebellum was removed, and the hemispheres were separated. The basal ganglia, meninges, and hippocampal formations were removed, leaving only the cortex area. The cortexes were then dissociated mechanically with a pipette in 4.5 g/L glucose Dulbecco's Modified Eagles Medium (DMEM, Gibco, Paisley, UK) supplemented with 10% (vol/vol) fetal bovine serum (FBS, Gibco, Paisley, UK), 0.01% antibiotic/antimycotic (100 U/mL penicillin, 0.25 μg/mL amphotericin B and 100 μg/mL streptomycin, Sigma, Steinheim, Germany) solution and 0.01% glutamine (Gibco, Paisley, UK) at 37°C. The dissociated cells were filtered through a 230 μm pore mesh and a 70 μm mesh (BD Falcon, Erembodegem, Belgium). After each filtration, the cells underwent two centrifugations at $200g \times 10$ min at room temperature (RT). After each centrifugation, the supernatant was discarded, and the pellet was resuspended in a fresh DMEM-supplemented medium. Cells were plated in a T-75 flask for Ca^{2+} experiments. To reduce the microglia contamination, cultures underwent horizontal agitation (McCarthy & De Vellis, 1980). After 6 days in culture (DIC), the T-75 flasks were agitated horizontally at 300 rpm for 4–5 h, and on DIC7, T-75 flasks

were agitated at 300 rpm for 4–5 h, and next cells from T-75 flasks were replated in 8-well plate for the Ca^{2+} imaging experiments and PLA assays in a 1:7 dilution in supplemented DMEM. Cells were kept in a humified atmosphere (5% CO_2) at 37°C. The culture medium was changed on DIC 3 and every 7 days after culture. Each culture was obtained using 5–7 Sprague Dawley pups.

5.7 | Cell culture

HEK-293T cells were grown in Dulbecco's modified Eagle's medium supplemented with 2 mM l-glutamine, 100 U/mL penicillin/streptomycin, and 10% (vol/vol, FBS, Invitrogen, USA) at 37°C and in an atmosphere of 5% CO_2. These cells were used to evaluate the D1R-CB1R complex expression.

5.8 | Bioluminescence resonance energy transfer (BRET) assays

For BRET assays, primary astrocytic cell cultures were transiently co-transfected with a constant amount of cDNA encoding for A_{2A}RRluc A_1RRLuc and with increasing amounts of cDNA corresponding to CB1RYFP. For the negative control, an equal amount of D1rRLuc and an increasing amount of CB1RYFP were used. Forty-eight hours after transfection cells were adjusted to 20 μg of protein using a Bradford assay kit (Bio-Rad, Munich, Germany) using bovine serum albumin for standardization. To quantify protein-YFP expression, fluorescence was read in a Mithras LB 940 equipped with a high-energy xenon flash lamp, using a 10 nm bandwidth excitation filter at 485 nm reading. For bioluminescence resonance energy transfer (BRET) measurements, readings were collected 1 min after the addition of 5 μM coelenterazine h (Molecular Probes, Eugene, OR) using a Mithras LB 940, which allows the integration of the signals detected in the short-wavelength filter at 485 nm and the long-wavelength filter at 530 nm. To quantify protein-Rluc expression, luminescence readings were performed (using a Mithras LB 940) 10 min after 5 μM coelenterazine h addition. The net BRET is defined as [(long-wavelength emission)/ (short-wavelength emission)]-Cf, where Cf corresponds to [(long-wavelength emission)/(short-wavelength emission)] for the donor construct expressed alone in the same experiment. GraphPad Prism software (San Diego, CA) was used to fit data. BRET is expressed as milli BRET units, mBU (net BRET × 1000).

5.9 | PLA assay

PLA assays were prepared as previously in Franco et al., 2019, with some mild modifications. Briefly, astrocytic primary cultures (19–21 DIC) grown on glass coverslips were fixed in 4% paraformaldehyde for 15 min, washed with PBS containing 20 mM glycine to quench the aldehyde groups, and permeabilized with the same buffer containing 0.05% Triton X-100 (5 min treatment). After 1 h incubation at 37°C

with blocking solution, cells were treated with specific antibodies against either A_{2A} or A1 receptors (rabbit anti-A_{2A}R-1/100- [Millipore, Darmstadt, Germany]; with mouse anti-A_1R-1/100- [Santa Cruz Technologies]). Cells were processed using the PLA probes detecting mouse and rabbit antibodies (Duolink II PLA probe anti-Rabbit plus and Duolink II PLA probe anti-Mouse minus) and nuclei were stained with Hoechst (1/200; Sigma-Aldrich). Coverslips were mounted using Mowiol solution. Samples were observed in a Leica SP2 confocal microscope (Leica Microsystems, Mannheim, Germany) equipped with an apochromatic ×63 oil-immersion objective (N.A. 1.4), and 405 and 561 nm laser lines. For each field of view a stack of two channels (one per staining) and 3 to 4 Z stacks with a step size of 1 μm were acquired. Quantification of cells containing one or more red spots versus total cells (blue nucleus) and, in cells containing spots, the ratio r (number of red spots/ cell), were determined by Duolink Image tool (Andy's Algorithm).

5.10 | _In vitro_ Ca^{2+} imaging

For the Ca^{2+} imaging experiments, 7 DIC astrocytes kept in T-75 flasks were seeded in 8 well Ibidi@ plates with a glass bottom (Ibidi GmbH, Martinsried, Germany) with 8 wells of 9.4 × 10.7 × 6.8 (mm). The Ibidi@ plates were previously coated with Poly-d-lysine (PDL) for 1 h and washed 3 times with sterile water. The 7 DIC astrocytes kept in T-75 flasks were trypsinized (1% trypsin–EDTA) for 1–2 min under agitation, and this reaction was stopped by the addition of 4.5 g/L glucose DMEM containing 10% fetal bovine serum with 0.01% antibiotic/antimycotic and glutamine. Until the day of the experiments (19–21 DIC), the plated cells were maintained in a suitable growing medium in a humidified atmosphere (5% CO2) at 37°C. On the day of the experiment, the cell medium was removed, and the cells were washed three times with external physiological solution Ca^{2+}-HEPES buffer (composition in mM: 125 NaCl, 1.25 NaH_2PO_4; 3 KCl; 10 D (+)-glucose; 2 $CaCl_2$; 2 $MgCl_2$ and 10 HEPES; pH 7.4 adjusted with NaOH). Before the experiment, cells were loaded with sensitive Ca^{2+} fluorescent dye FURA 2-acetoxymethyl, FURA-2 AM (5 μM), for 45 min at room temperature (Rose et al., 2003). Using a ratiometric dye has some advantages that other assays like single wavelength probes cannot offer like the ratio signal is independent of the dye concentration, and light intensity. These characteristics allow the evolution of intracellular Ca^{2+} to be determined independently of these artifacts. After FURA-2 AM incubation, the cells were washed once again with Ca^{2+}-HEPES buffer, three times. The Ibidi@ plates were mounted on an inverted microscope (Axiovert 135TV, Zeiss) with a xenon lamp and band-pass filters of 340 and 380 nm wavelengths. For the first set of experiments, cells were kept at 37°C in a humidified atmosphere, throughout the experiment. For the first 5 min of the assay, a Ca^{2+} baseline was established, and the tested drugs were applied directly in the medium. The CB1R agonist was applied 15 min after the antagonist in the same conditions. In all experiments, at 40 min, ionomycin (2 μM) was added. This Ca^{2+} ionophore in high concentrations can induce necrotic cell death (Montagne et al., 2015)

by a substantial increase of intracellular Ca^{2+}. This step allowed us to recognize which cells were viable during the assay. Only cells that responded to ionomycin through a substantial increase of ratio 340/380 nm were considered for statistical analysis. Image pairs were obtained every 5 or 10 s by exciting the preparations at 340 and 380 nm which were then used to obtain ratio images. In the second set of experiments, the CB1R receptor agonist was applied focally through a drug-filled micropipette placed under visual guidance over a single astroglial cell while all the other tested drugs were bath applied; CB1R receptor agonist release was made by focal pressure (15 psi for 3–10s) through a FemtoJet microinjector (Eppendorf, Hamburg, Germany), except where otherwise stated. Pressure application of external physiological solution did not cause any measurable change in intracellular Ca^{2+} concentration.

Excitation wavelengths were changed using a high-speed wavelength switcher, Lambda DG-4 (Sutter Instrument, Novato, CA, USA), and the emission wavelength was set to 510 nm. Image data were recorded by a CCD camera (Photometrics CoolSNAP fx) and processed and analyzed by the software MetaFluor (Universal Imaging, West Chester, PA, USA). Regions of interest were obtained by defining the profile of the cells and averaging the fluorescence intensity within the delimited area. Intensity values were converted to ratio 340/380 nm and all the values were normalized by the first ratio of each cell.

5.11 | *Ex vivo* Ca^{2+} imaging

Slices were placed in the microscope chamber and continuously superfused with ACSF containing 1 μM tetrodotoxin (Tocris Bioscience 1078). After a few minutes to allow tetrodotoxin perfusion, astrocytes were imaged with a CCD camera (Hamamatsu ORCA-R2 C10600) attached to an Olympus BX51WI upright microscope equipped with a 40X/0.80 W objective and CoolLED pE-100,470 nm illumination. Imaging was performed at one frame per second with 300 ms exposure time. The CCD camera and LED were controlled and synchronized with μManager software. GCaMP6f fluorescence was imaged for 60 s followed by a puff of 300 μM WIN-55212–2 in ACSF (3 s, 2 psi) delivered through a glass pipette (2–5 MΩ). Imaging continued up to 120 s after WIN-55212–2 application. In some cases, responding astrocytes were identified with a puff of 20 mM ATP.

Ca^{2+} imaging videos were analyzed with custom ImageJ (NIH), MATLAB (MathWorks), and R (The R Statistical Foundation) scripts. Bleaching was corrected with an exponential fit using the ImageJ plugin Bleach Correction. 8–15 regions of interest (ROIs) close to the puff pipette were drawn per slice and their average gray values measured over time. Signals were low-pass filtered (Chebyshev type II), discretized in 25-s bins, and the 20th percentile fit to a straight line to calculate background fluorescence (F_0). Final traces were calculated as change over basal ($\Delta F/F_0$) and smoothed with a Savitzky–Golay filter. Event peaks were detected at a $\Delta F/F_0$ threshold of two times the standard deviation and at least 0.25% change from baseline (0.0025 $\Delta F/F_0$ units). Peaks were defined as local maxima above the defined

threshold and separated by at least 3 s from any other event. Event frequency, mean amplitude, and mean duration were calculated per ROI and population measurements were calculated as the average of all ROIs per slice before and after WIN-55212-2 application.

5.12 | Extracellular recordings

5.12.1 | Extracellular fEPSPs recordings

Following the recovery period, slices were transferred to a recording chamber for submerged slices (1 mL capacity plus 5 mL dead volume) and were constantly superfused at a flow rate of 3 mL/min with aCSF kept at 32°C, gassed with 95% O_2/5%CO_2. Evoked field excitatory postsynaptic potentials (fEPSP) were recorded extracellularly by using a microelectrode (4 to 8 MΩ resistance) filled with aCSF solution placed in layer V of the mPFC area. fEPSP data were acquired using an Axoclamp-2B amplifier (Axon Instruments, Foster City, CA). fEPSPs were evoked by stimulation through a concentric electrode placed in layer II/III of the mPFC. Each stimulus consisted of a 0.1 ms rectangular pulse applied once every 20 s, except otherwise indicated. Averages of three consecutive responses were continuously acquired, digitized with the WinLTP program (Anderson & Collingridge, 2001), and quantified as the slope of the initial phase of the averaged fEPSPs. The stimulus intensity was adjusted at the beginning of the experiment to obtain a fEPSP slope that corresponds to about 50% of the maximal fEPSP slope.

5.12.2 | Long-term potentiation induction

LTP was induced in the mPFC as previously in the lab (Tanqueiro et al., 2021) by delivering a high-frequency stimulus (HFS) of one train of 100 Hz (50 pulses and 0.5 s duration) stimuli for priming, followed 15 min later by an HFS of four trains of 100 Hz (50 pulses, 0.5 s duration, and one every 10 s) stimuli. LTP was quantified as the percentage change in the average slope of the fEPSPs taken from 40 to 50 min after LTP induction relative to the average fEPSP slope measured during the 10 min prior to LTP induction. The effect of the drugs on LTP magnitude was evaluated by comparing the LTP magnitude in the control condition (aCSF superfusion) and drug condition (drug-tested superfusion). The used drugs remained in the bath until the end of the recording period.

5.12.3 | mIPSCs recordings

Individual slices were fixed with a grid in a recording chamber of about 1-mL volume and were continuously superfused by a gravitational system at 2–3 mL/min with aCSF at 30–32°C. Patch pipettes were made from borosilicate glass capillaries (1.5-mm outer diameter, 0.86 inner diameter, Harvard Apparatus, Holliston, MA, USA) and had a resistance of 4–9 MΩ when filled with an internal solution

containing (mM) the following: CsCl 125; NaCl 8; CaCl2 1; EGTA 10; HEPES 10; glucose 10; MgATP 5; NaGTP 0.4; and pH 7.2, adjusted with CsOH (50 wt% in H_2O), 280–290 Osm. Whole-cell recordings were obtained from pyramidal cells located at layer V. The cells were visualized with a microscope (Zeiss Axioskop 2FS, Jena, Germany) equipped with infrared video microscopy and differential interference contrast optics. All recordings were performed in voltage-clamp mode (VH = −70 mV) at 30–32°C with an Axopatch 200B (Molecular Devices) amplifier, under the control of pClamp10 software (Molecular Devices). Before the gigaseal formation, the offset potentials were nulled. Immediately after having whole-cell access, the membrane potential of the neurons was measured in current clamp mode (VH approximately −70 mV). Through all the recordings, the holding current was constantly monitored, and if it varied by more than 20%, the experiment would be rejected. Data were low-pass filtered using a 3- and 10-kHz three-pole Bessel filter, digitized at 5 Hz, and registered by the Clampex Software version 10.2 (Molecular Devices, Sunnyvale, CA, USA). Recordings were performed using the internal solution previously described plus 1 mM QX-314, a voltage-gated Na + channel blocker. During all recordings, aCSF was supplemented with kynurenic acid (Kyn, 1 mM), to block glutamate receptors. mIPSCs were recorded in aCSF supplemented with tetrodotoxin (TTX, 0.5 μM) and Kyn (1 mM). Miniature event analysis was performed using the MiniAnalysis software (Synaptosoft, GA, USA), with the amplitude threshold for event detection being set at 5× the average RMS noise. The rise time was calculated by finding the first data point to the left of the peak that shows 0.5% of the peak amplitude and subtracting the time at this point from the time at the peak. The decay time was calculated by finding the first data point to the right of the peak that shows 10% of the peak amplitude and taking a difference between the time at this point and the time at the peak. mIPSC frequency and amplitude were analyzed for 40 s every 2 min in order to obtain their time course variances. Statistical differences were assessed between IP3R2WT and IP3R2KO.

5.13 | Drugs

The following drugs were used: Ethyleneglycol bis(β-aminoethylester)-N,N,N′,N′-tetraacetate (EGTA) were obtained from Sigma (St. Louis, USA); arachidonyl-2′-chloroethylamide (ACEA), α-cyclopiazonic acid (α-CPA), 2-(2-FURAnyl)-7-(2-phenylethyl)-7H-pyrazolo[4,3-e][1,2,4]triazolo[1,5-c]pyrimidin-5-amine (SCH58261), 4-[2-[[6-Amino-9-(N-ethyl-β-D-riboFURAnuronamidosyl)-9H-purin-2-10yl]amino]ethyl] ben-zenepropanoic acid hydrochloride (CGS21680) and 1–6-[[(17β)-3-methoxyestra-1,3,5(10)-trien-17-yl]amino]hexyl-1H-pyrrole-2,5-dione (U73122), N^6-cyclopentyladenosine (CPA), 8-cyclopentyl-1,3-dipropylxanthine (DPCPX), N-(piperidin-1-yl)-5-(4-iodophenyl)-1-(2,4-dichlorophenyl)-4-methyl-1H-pyrazole-3-carboxamide (AM251) N-(2,6-Dimethylphenylcarbamoyl-methyl)triethylammonium bromide (QX-314) and (R)-(+)-[2,3-Dihydro-5-methyl-3-(4-morpholinylmethyl)pyrrolo[1,2,3-de]-1,4-benzoxazin-6-yl]-1-naphthalenylmethanone mesylate (WIN-55,212) were purchased from Tocris (Avonmouth, UK); 5-Oxazolecarboxylic acid, 2-(6-(bis(2-

((acetyloxy)methoxy)-2-oxoethyl)amino)-5-(2-(bis(2-((acetyloxy)meth-oxy)-2-oxoethyl)amino)-5-methylphenoxy)ethoxy)-2- benzoFURAnyl-, (acetyloxy)methyl ester 108964-32-5 (FURA-2AM) was obtained from Thermo Fisher (Massachusetts). ADA (E.C. 3.5.4.4, 200 U/mg in 50% glycerol (vol/vol), 10 mM potassium phosphate) was acquired from Roche. Stock solutions of drugs were prepared with dimethylsulphox-ide or distilled water or ethanol and kept at −20°C until used. Drugs' solutions were prepared from stock solutions diluted in either culture medium and/or incubation buffer immediately before use.

5.14 | Statistical analysis

All statistical analyses of presented data were performed using Graph-Pad Prism 5 (San Diego, CA, USA) software. Data are represented as mean ± standard error of the mean (SEM) of *n* independent observations (independent cultures or slices from different mice) in each experimental group. Two-sample comparisons were made using Student's *t* tests and multiple comparisons were made using one-way analysis of variance (ANOVA), followed by Bonferroni post-test. Statistical tests to determine the sample size were not applied. The investigators were not blinded in this study. Outliers were detected using the 1.5 IQR method.

DATA AVAILABILITY STATEMENT
The data that support the findings of this study are available from the corresponding author upon reasonable request.

ORCID

Joana Gonçalves-Ribeiro https://orcid.org/0000-0002-5194-6512
Oksana K. Savchak https://orcid.org/0000-0003-0448-5343
Sara Costa-Pinto https://orcid.org/0000-0002-9785-8956
Joana I. Gomes https://orcid.org/0000-0001-7761-1983
Rafael Rivas-Santisteban https://orcid.org/0000-0002-2078-6819
Javier Sánchez Romero https://orcid.org/0009-0002-4961-2465
Ana M. Sebastião https://orcid.org/0000-0001-9030-6115
Marta Navarrete https://orcid.org/0000-0003-2097-4788
Gemma Navarro https://orcid.org/0000-0003-4654-0873
Rafael Franco https://orcid.org/0000-0003-2549-4919
Sandra H. Vaz https://orcid.org/0000-0003-4258-9397

REFERENCES

Abreu, D. S., Gomes, J. I., Ribeiro, F. F., Diógenes, M. J., Sebastião, A. M., & Vaz, S. H. (2023). Astrocytes control hippocampal synaptic plasticity through the vesicular-dependent release of D-serine. *Frontiers in Cellular Neuroscience*, 17, 1282841.

Agostinho, P., Madeira, D., Dias, L., Simões, A. P., Cunha, R. A., & Canas, P. M. (2020). Purinergic signaling orchestrating neuron-glia communication. *Pharmacological Research*, 162, 105253.

Agulhon, C., Fiacco, T. A., & McCarthy, K. D. (2010). Hippocampal short- and long-term plasticity are not modulated by astrocyte Ca2+ signaling. *Science (80-)*, 327, 1250–1254.

Alloisio, S., Cugnoli, C., Ferroni, S., & Nobile, M. (2004). Differential modulation of ATP-induced calcium signalling by A1 and A2 adenosine receptors in cultured cortical astrocytes. *British Journal of Pharmacology*, 141, 935–942. https://doi.org/10.1038/sj.bjp.0705707

Anderson, W. W., & Collingridge, G. L. (2001). The LTP Program: A data acquisition program for on-line analysis of long-term potentiation and other synaptic events. *Journal of Neuroscience Methods*, 108, 71–83.

Araque, A., Carmignoto, G., Haydon, P. G., Oliet, S. H. R., Robitaille, R., & Volterra, A. (2014). Gliotransmitters travel in time and space. *Neuron*, 81, 728–739.

Araque, A., Parpura, V., Sanzgiri, R. P., & Haydon, P. G. (1999). Tripartite synapses: Glia, the unacknowledged partner. *Trends in Neurosciences*, 22, 208–215.

Ataka, T., & Gu, J. G. (2006). Relationship between tonic inhibitory currents and phasic inhibitory activity in the spinal cord lamina II region of adult mice. *Molecular Pain*, 2, 36.

Bambico, F. R., Katz, N., Debonnel, G., & Gobbi, G. (2007). Cannabinoids elicit antidepressant-like behavior and activate serotonergic neurons through the medial prefrontal cortex. *The Journal of Neuroscience*, 27, 11700–11711.

Banasr, M., & Duman, R. S. (2008). Glial loss in the prefrontal cortex is sufficient to induce depressive-like behaviors. *Biological Psychiatry*, 64, 863–870.

Baraibar, A. M., Belisle, L., Marsicano, G., Matute, C., Mato, S., Araque, A., & Kofuji, P. (2023). Spatial organization of neuron–astrocyte interactions in the somatosensory cortex. *Cerebral Cortex*, 33, 4498–4511.

Basavarajappa, B. S., Nagre, N. N., Xie, S., & Subbanna, S. (2014). Elevation of endogenous anandamide impairs LTP, learning, and memory through CB1 receptor signaling in mice. *Hippocampus*, 24, 808–818.

Batalha, V. L., Pego, J. M., Fontinha, B. M., Costenla, A. R., Valadas, J. S., Baqi, Y., Radjainia, H., Müller, C. E., Sebastião, A. M., & Lopes, L. V. (2012). Adenosine A2A receptor blockade reverts hippocampal stress-induced deficits and restores corticosterone circadian oscillation. *Molecular Psychiatry*, 18(3), 320–331. https://doi.org/10.1038/mp.2012.8

Blum, S., Hebert, A. E., & Dash, P. K. (2006). A role for the prefrontal cortex in recall of recent and remote memories. *Neuroreport*, 17, 341–344.

Bohme, G. A., Laville, M., Ledent, C., Parmentier, M., & Imperato, A. (1999). Enhanced long-term potentiation in mice lacking cannabinoid CB1 receptors. *Neuroscience*, 95, 5–7.

Boison, D. (2008). The adenosine kinase hypothesis of epileptogenesis. *Progress in Neurobiology*, 84, 249–262.

Boison, D. (2016). Adenosinergic signaling in epilepsy. *Neuropharmacology*, 104, 131–139.

Borea, P. A., Gessi, S., Merighi, S., Vincenzi, F., & Varani, K. (2018). Pharmacology of adenosine receptors: The state of the art. *Physiological Reviews*, 98, 1591–1625.

Borroto-Escuela, D. O., Hagman, B., Woolfenden, M., Pinton, L., Jiménez-Beristain, A., Oflijan, J., Narvaez, M., Di Palma, M., Feltmann, K., Sartini, S., Ambrogini, P., Ciruela, F., Cuppini, R., & Fuxe, K. (2016). In situ proximity ligation assay to study and understand the distribution and balance of GPCR homo- and heteroreceptor complexes in the brain. *NeuroMethods*, 110, 109–124. https://doi.org/10.1007/978-1-4939-3064-7_9

Brockett, A. T., Kane, G. A., Monari, P. K., Briones, B. A., Vigneron, P. A., Barber, G. A., Bermudez, A., Dieffenbach, U., Kloth, A. D., Buschman, T. J., & Gould, E. (2018). Evidence supporting a role for astrocytes in the regulation of cognitive flexibility and neuronal oscillations through the Ca2+ binding protein S100β. *PLoS One*, 13, e0195726. https://doi.org/10.1371/journal.pone.0195726

Carriba, P., Ortiz, O., Patkar, K., Justinova, Z., Stroik, J., Themann, A., Müller, C., Woods, A. S., Hope, B. T., Ciruela, F., Casadó, V., Canela, E. I., Lluis, C., Goldberg, S. R., Moratalla, R., Franco, R., & Ferré, S. (2007). Striatal adenosine A2A and cannabinoid CB1 receptors form functional heteromeric complexes that mediate the motor effects of cannabinoids. *Neuropsychopharmacology*, 32, 2249–2259.

Chevaleyre, V., Takahashi, K. A., & Castillo, P. E. (2006). Endocannabinoid-mediated synaptic plasticity in the CNS. *Annual Review of Neuroscience*, 29, 37–76. https://doi.org/10.1146/annurev.neuro.29.051605.112834

Chiodi, V., Ferrante, A., Ferraro, L., Potenza, R. L., Armida, M., Beggiato, S., Pèzzola, A., Bader, M., Fuxe, K., Popoli, P., & Domenici, M. R. (2016). Striatal adenosine-cannabinoid receptor interactions in rats overexpressing adenosine A2A receptors. *Journal of Neurochemistry*, 136, 907–917.

Cho, W. H., Noh, K., Lee, B. H., Barcelon, E., Jun, S. B., Park, H. Y., & Lee, S. J. (2022). Hippocampal astrocytes modulate anxiety-like behavior. *Nature Communications*, 13, 36344520.

Ciruela, F., Casadó, V., Rodrigues, R. J., Luján, R., Burgueño, J., Canals, M., Borycz, J., Rebola, N., Goldberg, S. R., Mallol, J., Cortés, A., Canela, E. I., López-Giménez, J. F., Milligan, G., Lluis, C., Cunha, R. A., Ferré, S., & Franco, R. (2006). Presynaptic control of striatal glutamatergic neurotransmission by adenosine A1-A2A receptor heteromers. *The Journal of Neuroscience*, 26, 2080–2087.

Corkrum, M., Covelo, A., Lines, J., Bellocchio, L., Pisansky, M., Loke, K., Quintana, R., Rothwell, P. E., Lujan, R., Marsicano, G., Martin, E. D., Thomas, M. J., Kofuji, P., & Araque, A. (2020). Dopamine-evoked synaptic regulation in the nucleus accumbens requires astrocyte activity. *Neuron*, 105(6), 1036–1047.e5. https://doi.org/10.1016/j.neuron.2019.12.026

Covelo, A., & Araque, A. (2018). Neuronal activity determines distinct gliotransmitter release from a single astrocyte. *eLife*, 7, 29380725.

Cristóvão-Ferreira, S., Navarro, G., Brugarolas, M., Pérez-Capote, K., Vaz, S. H., Fattorini, G., Conti, F., Lluis, C., Ribeiro, J. A., McCormick, P. J., Casadó, V., Franco, R., & Sebastião, A. M. (2013). A1R-A2AR heteromers coupled to Gs and Gi/0 proteins modulate GABA transport into astrocytes. *Purinergic Signal*, 9, 433–449.

Cunha, R. A., Correia-de-Sá, P., Sebastião, A. M., & Ribeiro, J. A. (1996). Preferential activation of excitatory adenosine receptors at rat hippocampal and neuromuscular synapses by adenosine formed from released adenine nucleotides. *British Journal of Pharmacology*, 119, 253–260.

Cunha, R. A., Vizi, E. S., Ribeiro, J. A., & Sebastião, A. M. (1996). Preferential release of ATP and its extracellular catabolism as a source of adenosine upon high- but not low-frequency stimulation of rat hippocampal slices. *Journal of Neurochemistry*, 67, 2180–2187. https://doi.org/10.1046/j.1471-4159.1996.67052180.x

de Ceglia, R., Ledonne, A., Litvin, D. G., Lind, B. L., Carriero, G., Latagliata, E. C., Bindocci, E., Di Castro, M. A., Savtchouk, I., Vitali, I., Ranjak, A., Congiu, M., Canonica, T., Wisden, W., Harris, K., Mameli, M., Mercuri, N., Telley, L., & Volterra, A. (2023). Specialized astrocytes mediate glutamatergic gliotransmission in the CNS. *Nature*, 622, 120–129.

Delicado, E. G., Rodrigues, A., Sen, R. P., Sebastiao, A. M., Ribeiro, J. A., & Miras-Portugal, M. T. (1990). Effect of 5′-(N-Ethylcarboxamido)adenosine on adenosine transport in cultured chromaffin cells. *Journal of Neurochemistry*, 54(6), 1941–1946. https://doi.org/10.1111/j.1471-4159.1990.tb04895.x

De Mendonça, A., & Ribeiro, J. A. (1994). Endogenous adenosine modulates long-term potentiation in the hippocampus. *Neuroscience*, 62, 385–390.

Di Castro, M. A., Chuquet, J., Liaudet, N., Bhaukaurally, K., Santello, M., Bouvier, D., Tiret, P., & Volterra, A. (2011). Local Ca2+ detection and modulation of synaptic release by astrocytes. *Nature Neuroscience*, 14, 1276–1284.

Durkee, C., & Alfonso, A. (2019). Diversity and specificity of astrocyte-neuron communication. *Neuroscience*, 396, 73–78.

Düster, R., Prickaerts, J., & Blokland, A. (2014). Purinergic signaling and hippocampal long-term potentiation. *Current Neuropharmacology*, 12, 37–43.

Euston, D. R., Gruber, A. J., & McNaughton, B. L. (2012). The role of medial prefrontal cortex in memory and decision making. *Neuron*, 76, 1057–1070.

Fénelon, K., Mukai, J., Xu, B., Hsu, P. K., Drew, L. J., Karayiorgou, M., Fischbach, G. D., MacDermott, A. B., & Gogos, J. A. (2011). Deficiency of Dgcr8, a gene disrupted by the 22q11.2 microdeletion, results in altered short-term plasticity in the prefrontal cortex. *Proceedings of the National Academy of Sciences of the United States of America*, 108, 4447–4452. https://doi.org/10.1073/pnas.1101219108

Ferré, S., Lluís, C., Justinova, Z., Quiroz, C., Orru, M., Navarro, G., Canela, E. I., Franco, R., & Goldberg, S. R. (2010). Adenosine-cannabinoid receptor interactions. Implications for striatal function. *British Journal of Pharmacology*, 160, 443–453.

Ferré, S., & Sebastião, A. M. (2016). Dissecting striatal adenosine-cannabinoid receptor interactions. New clues from rats overexpressing adenosine A2A receptors. *Journal of Neurochemistry*, 136, 897–899.

Ferreira, S. G., Gonçalves, F. Q., Marques, J. M., Tomé, R., Rodrigues, R. J., Nunes-Correia, I., Ledent, C., Harkany, T., Venance, L., Cunha, R. A., & Köfalvi, A. (2015). Presynaptic adenosine a 2A receptors dampen cannabinoid CB 1 receptor-mediated inhibition of corticostriatal glutamatergic transmission. *British Journal of Pharmacology*, 172, 1074–1086.

Forghani, R., & Krnjević, K. (1995). Adenosine antagonists have differential effects on induction of long-term potentiation in hippocampal slices. *Hippocampus*, 5, 71–77.

Franco, R., Reyes-Resina, I., Aguinaga, D., Lillo, A., Jiménez, J., Raïch, I., Borroto-Escuela, D. O., Ferreiro-Vera, C., Canela, E. I., Sánchez de Medina, V., del Ser-Badia, A., Fuxe, K., Saura, C. A., & Navarro, G. (2019). Potentiation of cannabinoid signaling in microglia by adenosine A2A receptor antagonists. *Glia*, 67, 2410–2423.

Fredholm, B. B., Chen, J. F., Cunha, R. A., Svenningsson, P., & Vaugeois, J. M. (2005). Adenosine and brain function. *International Review of Neurobiology*, 63, 191–270.

Gabbott, P. L. A., Warner, T. A., Jays, P. R. L., Salway, P., & Busby, S. J. (2005). Prefrontal cortex in the rat: Projections to subcortical autonomic, motor, and limbic centers. *The Journal of Comparative Neurology*, 492, 145–177.

Gemperle, A. Y., Enz, A., Pozza, M. F., Lüthi, A., & Olpe, H. R. (2003). Effects of clozapine, haloperidol and iloperidone on neurotransmission and synaptic plasticity in prefrontal cortex and their accumulation in brain tissue: An in vitro study. *Neuroscience*, 117, 681–695.

Giménez-Llort, L., Masino, S. A., Diao, L., Fernández-Teruel, A., Tobeña, A., Halldner, L., & Fredholm, B. B. (2005). Mice lacking the adenosine A1 receptor have normal spatial learning and plasticity in the CA1 region of the hippocampus, but they habituate more slowly. *Synapse*, 57, 8–16.

Goenaga, J., Araque, A., Kofuji, P., & Moro, D. H. (2023). Calcium signaling in astrocytes and gliotransmitter release. *Frontiers in Synaptic Neuroscience*, 15, 1138577.

Gomes, J. I., Farinha-Ferreira, M., Rei, N., Gonçalves-Ribeiro, J., Ribeiro, J. A., Sebastião, A. M., & Vaz, S. H. (2021). Of adenosine and the blues: The adenosinergic system in the pathophysiology and treatment of major depressive disorder. *Pharmacological Research*, 163, 105363.

Gómez-Gonzalo, M., Navarrete, M., Perea, G., Covelo, A., Martín-Fernández, M., Shigemoto, R., Luján, R., & Araque, A. (2015). Endocannabinoids induce lateral long-term potentiation of transmitter release by stimulation of Gliotransmission. *Cerebral Cortex*, 25, 3699–3712. https://doi.org/10.1093/cercor/bhu231

Gonçalves, F. Q., Matheus, F. C., Silva, H. B., Real, J. I., Rial, D., Rodrigues, R. J., Oses, J. P., Silva, A. C., Gonçalves, N., Prediger, R. D., Tomé, Â. R., & Cunha, R. A. (2023). Increased ATP release and higher impact of adenosine A2A receptors on Corticostriatal plasticity in a rat model of Presymptomatic Parkinson's disease. *Molecular Neurobiology*, 60, 1659–1674.

Gordon, G. R. J., Baimoukhametova, D. V., Hewitt, S. A., Rajapaksha, W. R. A. K. J. S., Fisher, T. E., & Bains, J. S. (2005). Norepinephrine triggers release of glial ATP to increase postsynaptic efficacy. *Nature Neuroscience*, 8, 1078–1086.

Guerra-Gomes, S., Cunha-Garcia, D., Marques Nascimento, D. S., Duarte-Silva, S., Loureiro-Campos, E., Morais Sardinha, V., Viana, J. F., Sousa, N., Maciel, P., Pinto, L., & Oliveira, J. F. (2020). IP3R2 null mice display a normal acquisition of somatic and neurological development milestones. *European Journal of Neuroscience*, 54, 5673–5686. https://doi.org/10.1111/ejn.14724

Guerra-Gomes, S., Sousa, N., Pinto, L., & Oliveira, J. F. (2018). Functional roles of astrocyte calcium elevations: From synapses to behavior. *Frontiers in Cellular Neuroscience*, 0, 427.

Han, J., Kesner, P., Metna-Laurent, M., Duan, T., Xu, L., Georges, F., Koehl, M., Abrous, D. N., Mendizabal-Zubiaga, J., Grandes, P., Liu, Q., Bai, G., Wang, W., Xiong, L., Ren, W., Marsicano, G., & Zhang, X. (2012). Acute cannabinoids impair working memory through astroglial CB 1 receptor modulation of hippocampal LTD. *Cell*, 148, 1039–1050.

Hashmi, A. Z., Hakim, W., Kruglov, E. A., Watanabe, A., Watkins, W., Dranoff, J. A., & Mehal, W. Z. (2007). Adenosine inhibits cytosolic calcium signals and chemotaxis in hepatic stellate cells. *American Journal of Physiology. Gastrointestinal and Liver Physiology*, 292, 395–401. https://doi.org/10.1152/ajpgi.00208.2006

Hatashita, Y., Wu, Z., Fujita, H., Kumamoto, T., Livet, J., Li, Y., Tanifuji, M., & Inoue, T. (2023). Spontaneous and multifaceted ATP release from astrocytes at the scale of hundreds of synapses. *Glia*, 71, 2250–2265. https://doi.org/10.1002/glia.24392

Henneberger, C., Papouin, T., Oliet, S. H. R., & Rusakov, D. A. (2010). Long-term potentiation depends on release of D-serine from astrocytes. *Nature*, 463, 232–236.

Hoffman, A. F., Laaris, N., Kawamura, M., Masino, S. A., Lupica, C. R., Lupica, C., & Author, J. N. (2010). Control of cannabinoid CB1 receptor function on glutamate axon terminals by endogenous adenosine acting at A1 receptors. *The Journal of Neuroscience*, 30, 545–555.

Howlett, A. C. (2005). Cannabinoid receptor signaling. In *Cannabinoids* (pp. 53–79). Springer-Verlag.

Jacob, P. F., Vaz, S. H., Ribeiro, J. A., & Sebastião, A. M. (2014). P2Y1 receptor inhibits GABA transport through a calcium signalling-dependent mechanism in rat cortical astrocytes. *Glia*, *62*(8), 1211–1226.

Jiménez-Dinamarca, I., Reyes-Lizana, R., Lemunao-Inostroza, Y., Cárdenas, K., Castro-Lazo, R., Peña, F., Lucero, C. M., Prieto-Villalobos, J., Retamal, M. A., Orellana, J. A., & Stehberg, J. (2022). GABAergic regulation of Astroglial Gliotransmission through Cx43 hemichannels. *International Journal of Molecular Sciences*, *23*, 36362410.

Kanno, T., & Nishizaki, T. (2012). A(2a) adenosine receptor mediates PKA-dependent glutamate release from synaptic-like vesicles and Ca(2+) efflux from an IP(3)- and ryanodine-insensitive intracellular calcium store in astrocytes. *Cellular Physiology and Biochemistry*, *30*, 1398–1412.

Kerkhofs, A., Canas, P. M., Timmerman, A. J., Heistek, T. S., Real, J. I., Xavier, C., Cunha, R. A., Mansvelder, H. D., & Ferreira, S. G. (2018). Adenosine A2A receptors control glutamatergic synaptic plasticity in fast spiking interneurons of the prefrontal cortex. *Frontiers in Pharmacology*, *9*, 29615897.

Klugmann, M., Goepfrich, A., Friemel, C. M., & Schneider, M. (2011). AAV-mediated overexpression of the CB1 receptor in the mPFC of adult rats alters cognitive flexibility, social behavior, and emotional reactivity. *Frontiers in Behavioral Neuroscience*, *5*, 21808613.

Köfalvi, A., Moreno, E., Cordomí, A., Cai, N. S., Fernández-Dueñas, V., Ferreira, S. G., Guixà-González, R., Sánchez-Soto, M., Yano, H., Casadó-Anguera, V., Cunha, R. A., Sebastião, A. M., Ciruela, F., Pardo, L., Casadó, V., & Ferré, S. (2020). Control of glutamate release by complexes of adenosine and cannabinoid receptors. *BMC Biology*, *18*, 9. https://doi.org/10.1186/s12915-020-0739-0

Kofuji, P., & Araque, A. (2021). Astrocytes and behavior. *Annual Review of Neuroscience*, *44*, 49–67.

Lafourcade, M., Elezgarai, I., Mato, S., Bakiri, Y., Grandes, P., & Manzoni, O. J. (2007). Molecular components and functions of the endocannabinoid system in mouse prefrontal cortex. *PLoS One*, *2*, e709.

Lalo, U., Palygin, O., Rasooli-Nejad, S., Andrew, J., Haydon, P. G., & Pankratov, Y. (2014). Exocytosis of ATP from astrocytes modulates phasic and tonic inhibition in the neocortex. *PLoS Biology*, *12*, e1001747.

Lange, S. C., Bak, L. K., Waagepetersen, H. S., Schousboe, A., & Norenberg, M. D. (2012). Primary cultures of astrocytes: Their value in understanding astrocytes in health and disease. *Neurochemical Research*, *37*, 2569–2588.

Lauckner, J. E., Hille, B., & Mackie, K. (2005). The cannabinoid agonist WIN55,212-2 increases intracellular calcium via CB1 receptor coupling to Gq/11 G proteins. *Proceedings of the National Academy of Sciences of the United States of America*, *102*, 19144–19149.

Le Meur, K., Mendizabal-Zubiaga, J., Grandes, P., & Audinat, E. (2012). GABA release by hippocampal astrocytes. *Frontiers in Computational Neuroscience*, *6*, 59.

Lee, S., Yoon, B. E., Berglund, K., Oh, S. J., Park, H., Shin, H. S., Augustine, G. J., & Lee, C. J. (2010). Channel-mediated tonic GABA release from glia. *Science (80-)*, *330*, 790–796. https://doi.org/10.1126/science.1184334

Li, X., Zima, A. V., Sheikh, F., Blatter, L. A., & Chen, J. (2005). Endothelin-1-induced arrhythmogenic Ca2+ signaling is abolished in atrial myocytes of inositol-1,4,5-trisphosphate(IP3)-receptor type 2-deficient mice. *Circulation Research*, *96*, 1274–1281.

Lima, A., Sardinha, V. M., Oliveira, A. F., Reis, M., Mota, C., Silva, M. A., Marques, F., Cerqueira, J. J., Pinto, L., Sousa, N., & Oliveira, J. F. (2014). Astrocyte pathology in the prefrontal cortex impairs the cognitive function of rats. *Molecular Psychiatry*, *19*, 834–841.

Lopes, L. V., Cunha, R. A., & Ribeiro, J. A. (1999). Cross talk between A1 and A(2A) adenosine receptors in the hippocampus and cortex of young adult and old rats. *Journal of Neurophysiology*, *82*, 3196–3203. https://doi.org/10.1152/jn.1999.82.6.3196

Lopes, R. F., Gonçalves-Ribeiro, J., Sebastião, A. M., Meneses, C., & Vaz, S. H. (2023). *SIGAA: Signaling automated analysis: A new tool for Ca2+ signaling quantification using ratiometric Ca2+ dyes*. Signal, Image Video Process.

Marchi, M., Raiteri, L., Risso, F., Vallarino, A., Bonfanti, A., Monopoli, A., Ongini, E., & Raiteri, M. (2002). Effects of adenosine A1 and A2A receptor activation on the evoked release of glutamate from rat cerebrocortical synaptosomes. *British Journal of Pharmacology*, *136*, 434–440.

Martín, R., Bajo-Grañeras, R., Moratalla, R., Perea, G., & Araque, A. (2015). Circuit-specific signaling in astrocyte-neuron networks in basal ganglia pathways. *Science (80-)*, *349*, 730–734.

Martin-Fernandez, M., Jamison, S., Robin, L. M., Zhao, Z., Martin, E. D., Aguilar, J., Benneyworth, M. A., Marsicano, G., & Araque, A. (2017). Synapse-specific astrocyte gating of amygdala-related behavior. *Nature Neuroscience*, *20*, 1540–1548.

McCarthy, K. D., & De Vellis, J. (1980). Preparation of separate astroglial and oligodendroglial cell cultures from rat cerebral tissue. *The Journal of Cell Biology*, *85*, 890–902.

Mederos, S., Sánchez-Puelles, C., Esparza, J., Valero, M., Ponomarenko, A., & Perea, G. (2021). GABAergic signaling to astrocytes in the prefrontal cortex sustains goal-directed behaviors. *Nature Neuroscience*, *24*, 82–92.

Min, R., & Nevian, T. (2012). Astrocyte signaling controls spike timing–dependent depression at neocortical synapses. *Nature Neuroscience*, *15*, 746–753.

Montagne, R., Berbon, M., Doublet, L., Debreuck, N., Baranzelli, A., Drobecq, H., Leroy, C., Delhem, N., Porte, H., Copin, M.-C., Dansin, E., Furlan, A., & Tulasne, D. (2015). Necrosis- and apoptosis-related met cleavages have divergent functional consequences. *Cell Death & Disease*, *6*, e1769.

Moreno, E., Chiarlone, A., Medrano, M., Puigdellívol, M., Bibic, L., Howell, L. A., Resel, E., Puente, N., Casarejos, M. J., Perucho, J., Botta, J., Suelves, N., Ciruela, F., Ginés, S., Galve-Roperh, I., Casadó, V., Grandes, P., Lutz, B., Monory, K., … Guzmán, M. (2017). Singular location and signaling profile of adenosine A2A-cannabinoid CB1 receptor Heteromers in the dorsal striatum. *Neuropsychopharmacology*, *43*, 964–977.

Mouro, F. M., Batalha, V. L., Ferreira, D. G., Coelho, J. E., Baqi, Y., Müller, C. E., Lopes, L. V., Ribeiro, J. A., & Sebastião, A. M. (2017). Chronic and acute adenosine A2A receptor blockade prevents long-term episodic memory disruption caused by acute cannabinoid CB1 receptor activation. *Neuropharmacology*, *117*, 316–327.

Mouro, F. M., Köfalvi, A., André, L. A., Baqi, Y., Müller, C. E., Ribeiro, J. A., & Sebastião, A. M. (2019). Memory deficits induced by chronic cannabinoid exposure are prevented by adenosine A2AR receptor antagonism. *Neuropharmacology*, *155*, 10–21.

Navarrete, M., & Araque, A. (2008). Endocannabinoids mediate neuron-astrocyte communication. *Neuron*, *57*, 883–893.

Navarrete, M., & Araque, A. (2010). Endocannabinoids potentiate synaptic transmission through stimulation of astrocytes. *Neuron*, *68*, 113–126.

Navarrete, M., Perea, G., de Sevilla, D. F., Gómez-Gonzalo, M., Núñez, A., Martín, E. D., & Araque, A. (2012). Astrocytes mediate in vivo cholinergic-induced synaptic plasticity. *PLoS Biology*, *10*, e1001259.

Oliveira da Cruz, J. F., Robin, L. M., Drago, F., Marsicano, G., & Metna-Laurent, M. (2016). Astroglial type-1 cannabinoid receptor (CB1): A new player in the tripartite synapse. *Neuroscience*, *323*, 35–42.

Panatier, A., Vallée, J., Haber, M., Murai, K. K., Lacaille, J. C., & Robitaille, R. (2011). Astrocytes are endogenous regulators of basal transmission at central synapses. *Cell*, *146*, 785–798.

Pascual, O., Casper, K. B., Kubera, C., Zhang, J., Revilla-Sanchez, R., Sul, J. Y., Takano, H., Moss, S. J., McCarthy, K., & Haydon, P. G. (2005). Astrocytic purinergic signaling coordinates synaptic networks. *Science*, *310*, 113–116.

Perea, G., & Araque, A. (2005). Glial calcium signaling and neuron–glia communication. *Cell Calcium*, *38*, 375–382.

Perea, G., Gómez, R., Mederos, S., Covelo, A., Ballesteros, J. J., Schlosser, L., Hernández-Vivanco, A., Martín-Fernández, M., Quintana, R., Rayan, A., Díez, A., Fuenzalida, M., Agarwal, A., Bergles, D. E., Bettler, B., Manahan-Vaughan, D., Martín, E. D., Kirchhoff, F., & Araque, A. (2016). Activity-dependent switch of GABAergic inhibition into glutamatergic excitation in astrocyte-neuron networks. *eLife, 5,* 28012274.

Perea, G., Navarrete, M., & Araque, A. (2009). Tripartite synapses: Astrocytes process and control synaptic information. *Trends in Neurosciences, 32,* 421–431.

Petravicz, J., Fiacco, T. A., & McCarthy, K. D. (2008). Loss of IP3 receptor-dependent Ca2+ increases in hippocampal astrocytes does not affect baseline CA1 pyramidal neuron synaptic activity. *The Journal of Neuroscience, 28,* 4967–4973.

Pinto-Duarte, A., Coelho, J. E., Cunha, R. A., Ribeiro, J. A., & Sebastião, A. M. (2005). Adenosine A2A receptors control the extracellular levels of adenosine through modulation of nucleoside transporters activity in the rat hippocampus. *Journal of Neurochemistry, 93*(3), 595–604. https://doi.org/10.1111/j.1471-4159.2005.03071.x

Ribeiro, J. A., Sebastião, A. M., & De Mendonça, A. (2002). Adenosine receptors in the nervous system: Pathophysiological implications. *Progress in Neurobiology, 68,* 377–392.

Robin, L. M., Oliveira da Cruz, J. F., Langlais, V. C., Martin-Fernandez, M., Metna-Laurent, M., Busquets-Garcia, A., Bellocchio, L., Soria-Gomez, E., Papouin, T., Varilh, M., Sherwood, M. W., Belluomo, I., Balcells, G., Matias, I., Bosier, B., Drago, F., Van Eeckhaut, A., Smolders, I., Georges, F., ... Marsicano, G. (2018). Astroglial CB1 receptors determine synaptic D-serine Availability to enable recognition memory. *Neuron, 98,* 935–944.e5.

Rose, C. R., Blum, R., Pichler, B., Lepier, A., Kafitz, K. W., & Konnerth, A. (2003). Truncated TrkB-T1 mediates neurotrophin-evoked calcium signalling in glia cells. *Nature, 426,* 74–78.

Sherwood, M. W., Arizono, M., Hisatsune, C., Bannai, H., Ebisui, E., Sherwood, J. L., Panatier, A., Oliet, S. H. R., & Mikoshiba, K. (2017). Astrocytic IP$_3$ Rs: Contribution to Ca^{2+} signalling and hippocampal LTP. *Glia, 65,* 502–513.

Silva-Cruz, A., Carlström, M., Ribeiro, J. A., & Sebastião, A. M. (2017). Dual influence of endocannabinoids on long-term potentiation of synaptic transmission. *Frontiers in Pharmacology, 8,* 921.

Simpson, J. R., Snyder, A. Z., Gusnard, D. A., & Raichle, M. E. (2001). Emotion-induced changes in human medial prefrontal cortex: I. During cognitive task performance. *Proceedings of the National Academy of Sciences of the United States of America, 98,* 683–687. https://doi.org/10.1073/pnas.98.2.683

Skowrońska, K., Obara-Michlewska, M., Zielińska, M., & Albrecht, J. (2019). NMDA receptors in astrocytes: In search for roles in neurotransmission and astrocytic homeostasis. *International Journal of Molecular Sciences, 20,* 6358855.

Smith, R., Lane, R. D., Alkozei, A., Bao, J., Smith, C., Sanova, A., Nettles, M., & Killgore, W. D. S. (2018). The role of medial prefrontal cortex in the working memory maintenance of one's own emotional responses. *Scientific Reports, 8*(1), 1–15.

Sousa, V. C., Assaife-Lopes, N., Ribeiro, J. A., Pratt, J. A., Brett, R. R., & Sebastião, A. M. (2011). Regulation of hippocampal cannabinoid CB1 receptor actions by adenosine A1 receptors and chronic caffeine administration: Implications for the effects of Δ9-tetrahydrocannabinol on spatial memory. *Neuropsychopharmacology, 36,* 472–487.

Sousa, V. C., Ribeiro, J. A., & Sebastião, A. M. (2013). Caffeine and adenosine receptor modulation of cannabinoid influence upon cognitive function. *Journal of Caffeine Research, 3,* 85–95.

Srinivasan, R., Huang, B. S., Venugopal, S., Johnston, A. D., Chai, H., Zeng, H., Golshani, P., & Khakh, B. S. (2015). Ca2+ signaling in astrocytes from Ip3r2−/− mice in brain slices and during startle responses in vivo. *Nature Neuroscience, 185,* 708–717.

Tanqueiro, S. R., Mouro, F. M., Ferreira, C. B., Freitas, C. F., Fonseca-Gomes, J., Simões do Couto, F., Sebastião, A. M., Dawson, N., & Diógenes, M. J. (2021). Sustained NMDA receptor hypofunction impairs brain-derived neurotropic factor signalling in the PFC, but not in the hippocampus, and disturbs PFC-dependent cognition in mice. *Journal of Psychopharmacology, 35,* 730–743.

Vaz, S. H., Jørgensen, T. N., Cristóvão-Ferreira, S., Duflot, S., Ribeiro, J. A., Gether, U., & Sebastião, A. M. (2011). Brain-derived neurotrophic factor (BDNF) enhances gaba transport by modulating the trafficking of GABA transporter-1 (GAT-1) from the plasma membrane of rat cortical astrocytes. *The Journal of Biological Chemistry, 286,* 40464–40476.

Volterra, A., & Meldolesi, J. (2005). Astrocytes, from brain glue to communication elements: The revolution continues. *Nature Reviews. Neuroscience, 6,* 626–640.

Wieraszko, A., Goldsmith, G., & Seyfried, T. N. (1989). Stimulation-dependent release of adenosine triphosphate from hippocampal slices. *Brain Research, 485,* 244–250.

Xiong, Y., Sun, S., Teng, S., & Zhou, J. M. (2018). Ca2+-dependent and Ca2+-independent ATP release in astrocytes. *Frontiers in Molecular Neuroscience, 11,* 224.

SUPPORTING INFORMATION

Additional supporting information can be found online in the Supporting Information section at the end of this article.